Citation: Rexer, M. and C. Hirt (2015), Spectral analysis of the Earth's topographic potential via 2D-DFT – a new data-based degree variance model to degree 90,000. Journal of Geodesy 89(9), 887-909, doi: 10.1007/s00190-015-0822-4.

Spectral analysis of the Earth's topographic potential via 2D-DFT – a new data-based degree variance model to degree 90,000

Moritz Rexer[1]

[1] Institute for Astronomical and Physical Geodesy & Institute for Advanced Study, Technische Universität München

m.rexer@tum.de

Christian Hirt[2,1]

[2]The Institute for Geoscience Research & Western Australian Geodesy Group & Department of Spatial Sciences , Curtin University, Perth, Australia

[1] Institute for Astronomical and Physical Geodesy & Institute for Advanced Study, Technische Universität München

c.hirt@curtin.edu.au

Abstract

Classical degree variance models (such as Kaula's rule or the Tscherning-Rapp model) often rely on low-resolution gravity data, so are subject to extrapolation when used to describe the decay of the gravity field at short spatial scales. This paper presents a new degree variance model based on the recently published GGMplus near-global land areas 220 m resolution gravity maps (Hirt et al. 2013). We investigate and use a 2D-DFT (discrete Fourier transform) approach to transform GGMplus gravity grids into degree variances. The method is described in detail and its approximation errors are studied using closed-loop experiments. Focus is placed on tiling, azimuth averaging, and windowing effects in the 2D-DFT method and on analytical fitting of degree variances. Approximation errors of the 2D-DFT procedure on the (spherical harmonic) degree variance are found to be at the 10-20% level. The importance of the reference surface (sphere, ellipsoid or topography) of the gravity data for correct interpretation of degree variance spectra is highlighted. The effect of the underlying mass arrangement (spherical or ellipsoidal approximation) on the degree variances is found to be crucial at short spatial scales. A rule-of-thumb for transformation of spectra between spherical and ellipsoidal approximation is derived. Application of the 2D-DFT on GGMplus gravity maps yields a new degree variance model to degree 90,000. The model is supported by GRACE, GOCE, EGM2008 and forward-modelled gravity at 3 billion land points over all land areas within the SRTM data coverage, and provides gravity signal variances at the surface of the topography. The model yields omission errors of ~ 9 mGal for gravity (~1.5 cm for geoid effects) at scales of 10 km, ~ 4 mGal (~ 1 mm) at 2km-scales, and ~ 2 mGal (~ 0.2 mm) at 1km-scales.

Key words: Degree variance, omission error, discrete Fourier transform, ultra-high resolution gravity, GGMplus, spherical approximation, ellipsoidal approximation

1. Introduction

Much progress has been made in global gravity field determination with the dedicated satellite gravity field missions GRACE (e.g., Tapley et al. 2004) and GOCE (e.g., Pail et al. 2011). While these missions provide good global data coverage, their resolution is limited to spatial scales of ~80 km due to the gravity attenuation with altitude. The fine structure of the field is therefore usually retrieved from (a) terrestrial measurements (e.g., gravity anomalies or vertical deflections) and (b) from gravity forward modelling (i.e., computation of gravity effects from topographic mass models), particularly over areas devoid of terrestrial data (Pavlis et al. 2007, Hirt et al. 2010). Due to the fact that terrestrial measurements are neither homogeneously nor completely given on a global scale (e.g., Pavlis et al. 2012), gravity effects implied by the topographic masses are often considered as a means to increase the resolution of a gravity model.

With the help of integration techniques based on Newton's law of gravitation, digital elevation models along with mass-density assumptions can be used to approximate the gravity field at very short scales (e.g. scales of few hundreds of meters to tens of kilometers). Recently, this has been done on a near-global scale by Hirt et al. (2013) in the spatial domain. The authors provide *GGMplus* gravity maps for all land areas between 60 ° North and 56° South at 220 m ground resolution. The maps incorporate gravity from a combination of GRACE and GOCE satellite observations, terrestrial gravity data from EGM2008 (Pavlis et al. 2012) and topographic gravity effects beyond the 10 km-resolution of EGM2008. The gridded GGMplus gravity maps provide fairly complete information on the topography-generated gravity field over the continents at spatial scales of 10 km down to 220 m corresponding to spherical harmonic degree of about 90,000.

In order to examine topography-generated gravity signal strengths at different spatial scales, and to describe the decay of these signals as a function of the spatial scale, some spectral representation of the gravity field is required. This can be in terms of spherical harmonic coefficients (SHCs) or degree variance spectra (power law) describing the decay of the field as a function of wavelength. Three techniques suitable for this are:

- Global spherical harmonic analysis transforming gridded gravity data to SHCs (e.g., Pavlis et al. 2012, Gruber and Abrikosov 2014)
- Spectral-domain gravity forward modelling transforming a global spherical harmonic topographic mass model to SHCs of the implied potential (e.g., Rummel et al. 1988, Balmino et al. 2012)
- Application of 2D - Fourier techniques to derive degree variance spectra of gridded gravity data (e.g., Forsberg 1984a, Flury 2006), which is the scope of this paper.

While the first two methods have been applied to harmonic degree 10,800, or ~2 km spatial scales (Abrikosov et al. 2012, Balmino et al. 2012), there are currently no results from global harmonic analysis or spectral-domain forward modelling reported in the literature that reach sub-km resolution for degree variance spectra. This may be due to significant computational costs associated with ultra-high degree spherical harmonic modelling, particularly with the forward method that involves multiple harmonic analyses (e.g. Hirt and Kuhn 2014). However,

ultra-high resolution spectral representations would be useful to study the short-scale properties of the gravity field, e.g., to derive signal strengths and omission errors.

In this paper we determine degree variance spectra of the topographic potential at short spatial scales as incorporated in GGMplus (harmonic band of degrees 2161 to 90,000) with near-global scope using 2D - Fourier transform and variance model fitting techniques. At long spatial scales the spectra are supported by a combination of satellite gravity (GRACE and GOCE) and terrestrial gravity as contained in EGM2008 (harmonic band of degrees 2 to 2160). The spherical harmonic power spectra are computed from equi-angular GGMplus grids of gravity disturbances (http://ddfe.curtin.edu.au/models/GGMplus/). As a major advantage over spherical harmonic modelling, 2D – Fourier techniques can be flexibly applied on regional and global data sets to derive power spectra and are computationally less expensive than the first two methods when going to ultra-high degree. This is evident from the fact that 2D - Fourier techniques were used already few years ago to study the power spectra of local and regional gravity data sets to ultra-high degree (e.g. Flury 2006; Voigt and Denker 2007), cf. Section 2. Different to the first two techniques, 2D - Fourier methods do not yield sets of SHCs as spectral description of the gravity data set, and involve some approximations, which are studied and quantified in this paper. While potential spectra from 2D Fourier techniques and several degree variance models are reported in the literature, a guide that would describe and analyse all processing steps in detail and investigate the approximations involved and their impact on the estimated spectra, was not available to us.

This paper attempts to provide a tutorial-style description for the computation of degree variances and the consecutive fitting of degree variance models using commonly used mathematical models (Section 3). We make use of a two-dimensional *Discrete Fourier Transform* (DFT) approach dating back to Forsberg (1984a) for recovery of potential spectra. This approach is reviewed here and tested in a closed-loop environment in view of application on global and near-global gridded gravity data. We discuss in detail the so-called radial averaging in the 2D-DFT, and focus on the role of the reference surface for spherical harmonic spectra (sphere, ellipsoid or topography). This is rarely dealt with in the literature but crucial for interpretation of degree variances. We further develop a rule of thumb for the transformation of degree variances of the topographic potential from spherical to ellipsoidal approximation and vice versa. With the computed degree variances in hand we are able to define a new degree variance model based on GGMplus which describes the spectral energy of the topographic potential at the surface of the Earth's landmasses to ultra-fine spatial scales (Section 4).

Our work extends the study by Flury (2006) who analysed the signal strength of the medium-wavelength part of the gravity field. While Flury studied the spectral properties of topography-reduced gravity by 2D-DFT, he pointed out (in his outlook) the need for investigation of the very-short wavelength components caused by the topographic masses and computed from digital terrain models. This is exactly the purpose of this work.

This paper is structured as follows. In section 2 we start with some introductory comments on the topographic potential at short scales and its computation through forward modelling techniques. We describe the spherical harmonic modelling concept, elaborate the spherical

and ellipsoidal approximation regarding the underlying mass distribution of those models, and define degree variances. In section 3 we introduce the mathematical tools and experiments that are needed for the computation and correct interpretation of degree variances recovered from 2D grids of topographic gravity. We elaborate – in form of a detailed guide – the 2D-DFT approach of Forsberg (1984a) for its global application and discuss the different domains of degree variances (e.g., sphere vs. ellipsoid). Section 4 deals with the approximation of the topographic gravity energy to ultra-short scales of 220 m (equivalent to spherical harmonic degree 90000) based on GGMplus gravity maps, and omission errors are estimated. Further, we deal with the nature and the interpretation of the computed degree variance models based on spherical and ellipsoidal approximations. Finally, in Section 5 we summarise our findings and give an outlook on future work.

2. Background

2.1 Topographic potential and topographic gravity effects

Because of the quadratic attenuation of gravity with distance, the fine structure of the Earth's gravity field is strongly influenced by the mass distribution in the outermost layer of the Earth – the topography. While the Earth's flattening and the masses of core and mantle account for more than 99% of the total variations in gravity, the topographic masses cause less than 1% of the global variations (cf. Torge 2001). Locally and particularly in areas of rugged terrain, however, the topographic masses are necessary to explain the full gravitational signal because the contribution of the topography to gravity is dominant at very short scales. Since gravity observations on very short scales are limited, forward modelling of gravity effects is a crucial technique in view of generating high-resolution gravity field models (Pavlis et al. 2012; Hirt et al. 2013).

Besides the visible topographic masses, other components – such as mass anomalies in the Earth's interior, sediments, salt domes – also generate higher-frequency gravity signals. The gravity forward modeling data used in this study are based on the visible topographic masses as represented by the SRTM topography.

Forward gravity field modelling techniques can be classified as follows (Kuhn and Seitz 2005):

- Space domain techniques rely on numerical evaluation of Newton's law of gravitation to yield topographic gravity effects (e.g., Forsberg 1984b, Pavlis et al. 2007, Grombein et al. 2014),
- Spectral domain techniques expand the topographic potential into integer powers of topographic heights and require several harmonic analyses *or need some rigorous formulation* to obtain the SHCs of the topographic potential, and subsequent synthesis to derive gravity effects (e.g., Rummel et al. 1988, *Pavlis and Rapp 1990,* Novak 2010, Claessens and Hirt 2013).

For more details and an in-depth comparison of both forward modelling techniques we refer to Hirt and Kuhn (2014). Importantly, the approaches are often based on the assumption of an underlying mass sphere with topographic masses assumed to reside on Earth's spherical surface. The topographic gravity constituents of the GGMplus gravity maps which we

investigate in this study were generated in the space domain with the well-known residual terrain modelling (RTM) technique by Forsberg (1984b). GGMplus is based on a spherically approximated mass distribution as far as the topography-implied gravity signal (RTM) is concerned (see section 2.2) and a full account of the RTM forward modelling of GGMplus is given in Hirt et al. (2014).

The spectral characteristics of topographic gravity effects on short scales have been investigated in local and regional scale studies e.g., by Voigt and Denker (2007) and Jekeli (2010). Voigt and Denker (2007) investigated topographic gravity effects on gravity anomalies, deflections of the vertical and geoid heights computed from digital terrain models (DTM) with 1'', 3'', 6'', 12'' and 30'' (arc-second) resolution in Germany. Their tests concentrate on three 1° x 1° tiles for which empirical covariance functions and power spectral densities (and degree variances) are computed and analysed. In view of a one centimetre geoid they conclude that at least a 6'' DTM for an alpine region and 30'' DTMs for the non-alpine regions are required. Jekeli (2010) elaborated the disturbing gravity potential as a stochastic process and presents two topographic PSDs generated from 1 arc-min gravity anomaly grids over the mid US. The author analytically derived a linear relationship between the topographic heights and the gravity anomaly, which is confirmed empirically with digital elevation data of 30 arc-sec resolution over the same areas.

2.2 Spherical harmonic models, spherical vs. ellipsoidal approximation

Today, spherical harmonic (SH) representations are the most common way to globally describe the gravity field. Following Sanso and Sideris (2013), a global representation of the disturbing potential T may be written as

$$T(\theta,\lambda,r) = \frac{GM}{R} \sum_{l=2}^{L_{max}} \left(\frac{R}{r}\right)^{l+1} \sum_{m=-l}^{l} CS_{lm}\, Y_{lm}\,(\theta,\lambda)\,, \qquad (1)$$

where CS_{lm} are the SH coefficients of the representation, Y_{lm} are the SH basis functions, R is the scaling parameter associated with the model coefficients (often the semi-major axis *a* of some reference ellipsoid), GM is the product of the gravitational constant times the Earth's mass, l is the spherical harmonic degree and m is the spherical harmonic order, and *lmax* the maximum degree of expansion. Negative and positive orders m (m<0; m≥0) denote the affiliation to the sine and cosine terms of the base functions, respectively. The geocentric coordinate triplet – geocentric latitude, longitude and geocentric radius θ, λ, r - defines the point of evaluation of the series, usually located outside of the Earth's topographic masses. For more details on the spherical harmonic representation, see e.g. Sanso and Sideris (2013).

Spherical harmonic potential coefficients can be computed via forward modelling techniques from mass distributions on a sphere, or on an ellipsoid. In either case, the SH coefficients describe the potential field in the domain exterior to the mass distributions, where the field is harmonic.

Spherical harmonic models in *spherical approximation* are computed from masses arranged on the surface of a sphere of some constant radius. This requires "mapping" of the topography (e.g., taken from an elevation model) onto the surface of the sphere. This approach has been used, e.g., in Rummel (1988), Balmino et al. (2012), and Hirt and Kuhn (2012) to construct

models of Earth's topographic potential in spherical approximation. In this paper we use the topographic potential model dV_SPH_RET2012 (Hirt and Kuhn 2012) as an example for spherical harmonic models in spherical approximation. Besides Earth's visible topography it also models gravity effects of the ocean water masses, those of the major lakes and masses of Earth's ice sheets via the concept of rock-equivalent topography (e.g. Rummel et al. 1988). While models such as dV_SPH_RET2012 "disregard" the ellipsoidal shape of the Earth, they are useful e.g., for testing of computational procedures as will be shown in Section 3.

When gravity forward modelling is applied to a mass distribution arranged on the surface of some reference ellipsoid, the topographic potential is obtained in *ellipsoidal approximation* (Claessens and Hirt 2013, Grombein et al. 2014). An example for a SH model of the topographic potential in ellipsoidal approximation is the dV_ELL_RET2012 model (Claessens and Hirt 2013). In this type of model, the mass arrangement is much closer to that of the real Earth than in spherical approximation.

Spherical harmonic models of Earth's geopotential, e.g., those available via IAG's *International Centre for Global Earth Model* (ICGEM) service, are in ellipsoidal approximation too. This is because geopotential models are usually based on gravity field observations, which reflect that the field-generating mass distribution is – in good approximation – ellipsoidal. For instance, the EGM2008 geopotential model (Pavlis et al. 2012), those from the GOCE gravity field mission (Pail et al. 2011), among other geopotential models of the ICGEM, can be considered as ellipsoidal approximation – type.

In summary, the main difference between spherical harmonic potential models in spherical and ellipsoidal approximation in this study is the arrangement of the field-generating masses (sphere vs. ellipsoid), which come into play when forward modelling the gravitational field in spherical harmonics.

2.3 Degree variances

Degree variance models are power laws that describe the decay of the gravity signal in some spectral representation. They are mostly of purely empirical nature and reflect the observable variations in a set of global spherical harmonic coefficients (see section 2.2). As such degree variances are dimensionless (unit less). They are defined as the sum of squared spherical harmonic coefficients per spherical harmonic degree as

$$c_l^2 = \sum_{m=-l}^{l} CS_{lm}^2 \quad . \qquad (2)$$

In other words the degree variance of degree l reflects the signal power contained in all the coefficients of same degree (and of different orders $\mathrm{m} \in [-\mathrm{l}, \ldots, +\mathrm{l}]$). Degree variances as computed in this work refer to gravity disturbances and are given in mGal². They relate to dimensionless degree variances (Eq. 2) by the (functional-dependent) scaling factor Ψ (Table 1) following

$$c_l^2[\Psi] = \Psi \cdot \sum_{m=-l}^{l} CS_{lm}^2 \, , \qquad (3)$$

Note that the scalingfactors may be derived from the spherical harmonic expansion (of the respective gravity quantity) for r=R , i.e., converted degree variances (e.g. in metres or mGal) roughly reflect the signal strength (per wavelength) as obtained from a synthesis with evaluation points residing on the surface of a sphere of radius R.

Table 1 : Gravity functionals and degree variance dimensioning factors together with their unit; E: Eötvös

Gravity functional	**dimensioning factor Ψ**	**Unit**
None	1	-
N : geoid Heights	R^2	m^2
T_r: gravity disturbances	$(l+1)^2 \left(\frac{GM \cdot 10^5}{R^2}\right)^2$	$mGal^2$
Δg : gravity anomalies	$(l-1)^2 \left(\frac{GM \cdot 10^5}{R^2}\right)^2$	$mGal^2$

Degree variances generally can be obtained from

- a set of spherical harmonic coefficients: e.g., of gravity field models as found at the ICGEM and evaluated by Eq. 2.
- degree variance models/rules (based on analytical functions): e.g. Kaula (1966), Tscherning and Rapp (1974), Heller and Jordan (1976), Moritz (1977), Jekeli (1978), Flury (2006), Sanso and Sideris (2013), also see Sect. 3.2 and Sect. 4.

3 Recovering the spherical harmonic power spectrum from gridded gravity data by 2D-DFT

3.1 Computation of degree variances by 2D-DFT

In the literature, different ways for computing degree variances from a set of 2D-scattered point gravity values are described. Flury (2006) reviews several approaches to calculate degree variances and elaborates their complementarity (see Fig. 5 in Flury 2006). In principle one can either choose to estimate the degree variances from the 2D-PSDs (power spectral density) by azimuth averaging (c.f. Forsberg 1984a) or to calculate the degree variances from the empirical auto-covariance function (or from an analytical auto-covariance model, cf. Wenzel and Arabelos 1981). Both ways naturally assume homogeneity, isotropy and periodicity of the signals as well as no violations of the sampling theorem in the discretization process. With PSDs, the calculation of the Legendre polynomials can be omitted as the similarity of the shape of the Bessel functions and the Legendre polynomials is exploited (Forsberg, 1984a). The PSDs are generally obtained by Fourier transformation of an equally spaced grid calculated from the 2D-scattered point data. Note that PSDs can also be retrieved from the auto-covariance function of the 2D-scattered point data by the so-called discrete *Hankel transform* (c.f. Flury, 2006).

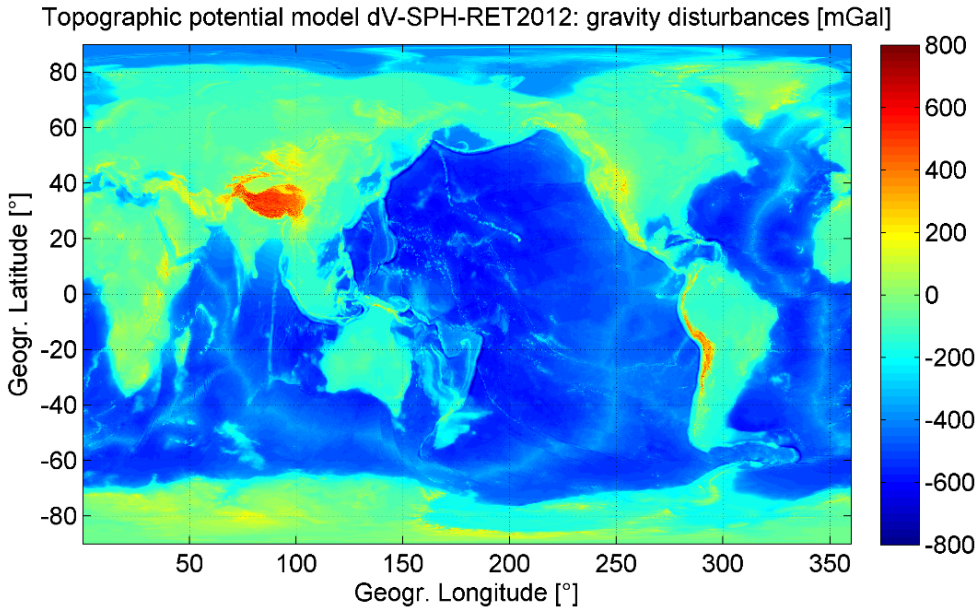

Figure 1: Global 5'x5' – gravity disturbance grid of the topographic potential model dV_SPH_RET2012 evaluated from degrees 0…2160 (Eq. 4)

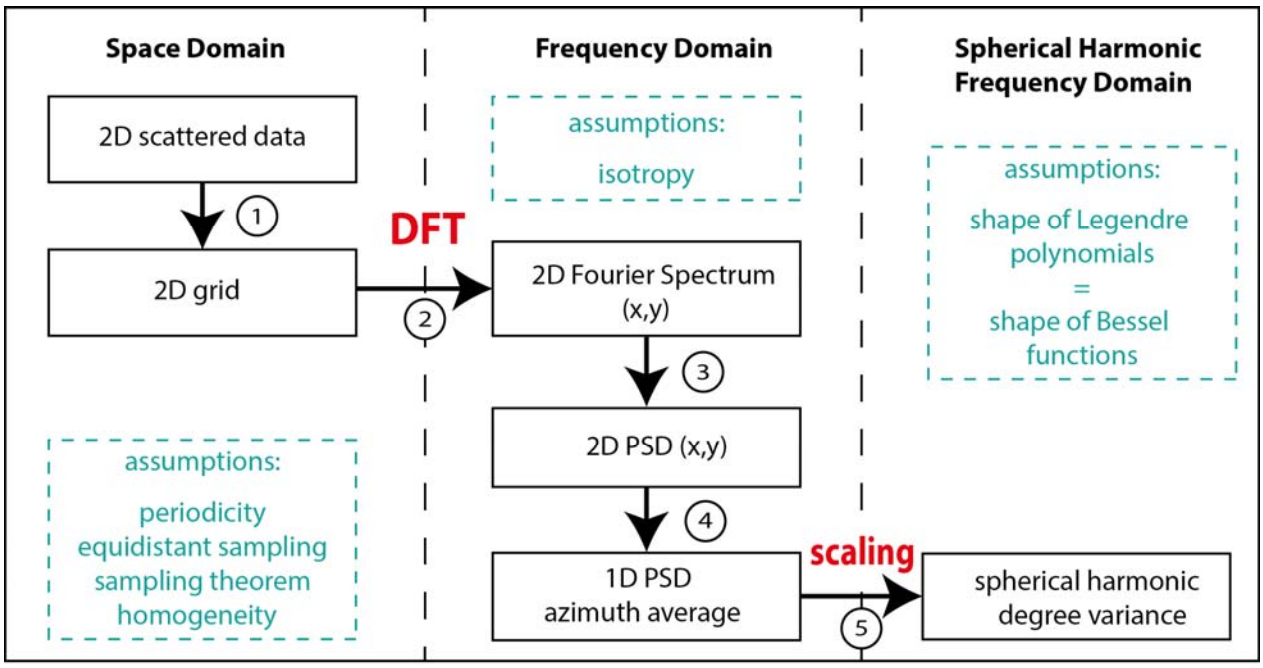

Figure 2: Flow chart showing the transition of gravity data in Space Domain to PSDs in Frequency Domain and to degree variances in Spherical Harmonic Frequency Domain

To exemplify the processing steps of the 2D-DFT method, we use a global 5 arc-min grid of topography-implied gravity disturbances (Fig. 1). These were synthesised from the spherical-harmonic topographic potential model dV-SPH-RET2012 (Hirt and Kuhn 2012, section 2.2) in the spectral band of harmonic degrees 0 to 2160 with the harmonic_synth software (Holmes and Pavlis 2008) following

$$\delta g(\theta,\lambda,r) = \frac{GM}{R^2} \sum_{l=2}^{L_{max}} (l+1) \left(\frac{R}{r}\right)^{l+1} \sum_{m=-l}^{l} CS_{lm}\, Y_{lm}(\theta,\lambda). \qquad (4)$$

The dV-SPH-RET2012 model is chosen in this study because it allows (i) computation of the true spectrum of potential degree variances to benchmark all approximation errors in the 2D-DFT method, and (ii) its approximation level is suitable for testing Forsberg's 2D-DFT formalism which is shown to be based on spherical approximation, too.

In Fig. 2 the flow from 2D-gridded data in *Space Domain* to the signal representation in *Frequency Domain* and finally the transformation to the *Spherical Harmonic Frequency Domain* is shown. Next a detailed description of the five working steps shown in Fig. 2 is given for the computation of degree variances. Following the procedure of Forsberg (1984a) and the description given in Flury (2006), the guide elaborates the details of the 2D Fourier transform for potential spectrum recovery.

1. Interpolation of 2D-scattered gravity data to an equidistant grid with K_x row-samples at the equidistant coordinates $x_k$and K_y column-samples at the equidistant coordinates y_j

$$x_k = k \cdot \Delta x \quad (5)$$
$$y_j = j \cdot \Delta y \quad (6)$$

where $k = 1,2 \dots K_x$, $j = 1,2 \dots K_y$ and Δx / Δy is the equidistant spacing of the grid in row- / column direction in metres. The equidistant sampling in metres is related to the spacing in degree by the mean co-latitude θ_{ave} of the grid following

$$\begin{Bmatrix} \Delta x\ [km] \\ \Delta y\ [km] \end{Bmatrix} = \begin{Bmatrix} \Delta x\ [rad] \\ \Delta y\ [rad] \cdot \sin\theta_{ave} \end{Bmatrix} \cdot R\ . \quad (7)$$

We acknowledge that according to the definition in Eq. 7 equidistant sampling is only given in good approximation for small grids, thus one DFT prerequisite is actually violated for regional or global grids. However, closed loop results will show this effect to be non-critical.

2. The discrete 2D Fourier transform of the gridded data *f (x,y)* is given by

$$F\left(v_p, v_q\right) = \frac{1}{K_x K_y} \sum_{k=0}^{K_x-1} \sum_{j=0}^{K_y-1} f\left(x_k, y_j\right) \cdot e^{-i2\pi\left(\frac{pk}{K_x}+\frac{qj}{K_y}\right)} \quad (8)$$

returning the 2-dimensional Fourier Spectrum *F* (v_p, v_q) at the frequencies v_p and v_q for $p = 0,1, \dots K_x - 1$ and $q = 0,1, \dots K_y - 1$. The Fourier Transform is complex-valued and can generally be described by a real and an imaginary part as

$$F\left(v_p, v_q\right) = a\left(v_p, v_q\right) - ib(v_p, v_q) \quad (9)$$

where *a* and *b* are the Fourier coefficients at the frequencies $v_p\ and\ v_q$.

3. The 2D-PSD is then estimated by

$$\phi(v_p, v_q) = D_x D_y \left|F(v_{p,} v_q)\right|^2, \tag{10}$$

as the square of the amplitude spectrum $\left|F(v_p v_q)\right|$, where

$$\left|F(v_p v_q)\right| = \sqrt{a^2(v_p, v_q) + b^2(v_p, v_q)}, \tag{11}$$

and scaled to the grid dimension $D_x = K_x \cdot \Delta x$ and $D_y = K_y \cdot \Delta y$. The frequencies are defined as $v_p = p/D_x$ in the row-direction and as $v_q = p/D_y$ in the column-direction (their unit is km^{-1}). Note that only the one-sided spectrum is of interest (corresponding to the upper left quadrant of the 2D Fourier Transform), as the 2D-PSD is mirrored at its centre. The unit of the PSD is $mGal^2 km^2$ for gravity anomalies. As example, Fig. 3 (left plot) shows the corresponding 2D-PSD of the previously introduced dV-SPH-RET2012 gravity disturbance grid, which exhibits the radial decay of the signal power with rising frequency and a sudden drop at $v_p = v_q \approx 0.1078\ km^{-1}$ which corresponds to the maximum harmonic degree (= 2160) of the model.

4. In order to obtain a 1D-PSD which later can be transformed to degree variances a so called "azimuth averaging" (Forsberg, 1984a) procedure is applied to the 2D-PSD. Values along equi-frequency circles (values at the same azimuth distance from the upper left corner of the PSD-matrix) are averaged, following

$$\phi(v_i) = \phi(\sqrt{v_p^2 + v_q^2}) \tag{12}$$

In other words, frequency classes V_i are to be defined containing the average PSD corresponding to the average frequency v_i within the class boundaries $V_i - \frac{\Delta h}{2} \leq \sqrt{v_p^2 + v_q^2} < V_i + \frac{\Delta h}{2}$, where Δh is the class width (Fig. 3, right plot). The parameter Δh then defines the spectral resolution of the approach and directly affects the smoothness of the computed degree variance curve (see step 5 and Fig. 4).

5. Finally, the obtained azimuth average $\phi(v_i)$ of the 2D-PSD is scaled to physically interpretable quantities related to the signal contained in the coefficients of a spherical harmonic representation of the gravitational potential. The transformation is given in Forsberg (1984b, p. 8-10) and is a good approximation especially for high spherical harmonic degrees (l>10). Hence, it is well suited to determine the signal at short spatial scales. It is based on the similarity of the shape of the Bessel functions J_0 and Legendre Polynomials P_l, as shown in Forsberg (1984a) : $P_l(\theta) \approx J_0(\frac{2l+1}{2} \cdot \theta)$ with a relative error of 1 % at $l = 10$ and $\theta = 8.1^\circ$. We investigated the approximation errors in detail for various degrees and latitudes. Our numerical investigations show that the

relative error of this approximation stays below 10 % for $\theta \leq 60^{\circ}$ and below 25 % for $\theta \leq 90^{\circ}$ up to degree 90000.

Degree variances c_l^2 are then (approximately) obtained by

$$c_l^2 \approx \frac{l+\frac{1}{2}}{2\,\pi\,R^2}\,\phi(v_i) \qquad (13)$$

where R is Earth's mean radius 6371008.77 m (c.f. Moritz 2000) and l denotes the spherical harmonic degree. The degree variances are defined for the "natural" wave numbers, which are the frequencies $v_i = (l+\frac{1}{2})/(R\pi)$. The frequencies v_i can easily be transformed to the corresponding spherical harmonic degree by the simple relation

$$l = (\pi R)\cdot v_i - \frac{1}{2}. \qquad (14)$$

The approach e.g. finds application in studies by Forsberg (1984a,1984b), Vassiliou and Schwarz (1987), Flury (2006), Voigt and Denker (2007), Jekeli (2010) and Szücs et al. (2014), where the high frequency part of the spherical harmonic power spectrum was retrieved from regional datasets.

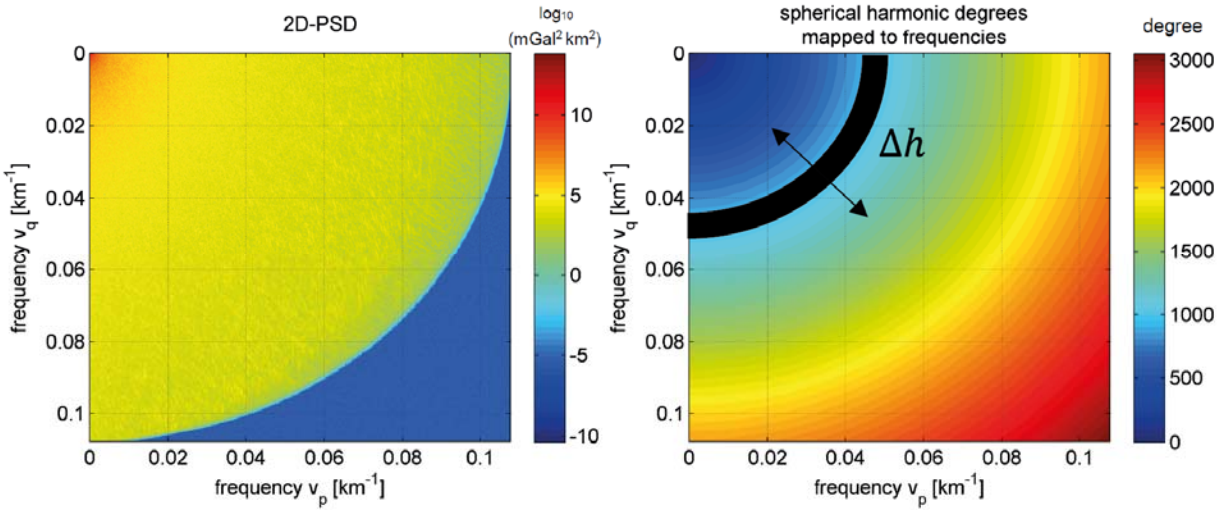

Figure 3 : Two-dimensional power spectrum density $\phi(v_p, v_q)$ in log10($mGal^2km^2$) (left) and the corresponding spherical harmonic degrees (right) of the Fourier Spectrum derived from a global 5'x5' dV_SPH_RET2012 grid evaluated from degrees 0…2160; the black illustration in the right plot shows the meaning of the class-width parameter Δh of the azimuth-averaging procedure

The minimum L_{min} and maximum L_{max} retrievable spherical harmonic degree depends on the dimension of the grid D_x and D_y and the sampling distance $\Delta_{\lambda,\varphi} = \Delta x = \Delta y$, respectively:

$$L_{max} = \frac{1}{\Delta_{\lambda,\varphi}\,[^{\circ}]}\cdot 180^{\circ} - 0.5 = \frac{1}{\Delta_{x,y}[km]}\cdot \pi R - \frac{1}{2} \qquad (15)$$

$$L_{min} = \frac{1}{D_{x,y}[^\circ]} \cdot 180^\circ - 0.5 = \frac{1}{D_{x,y}[km]} \cdot \pi R - \frac{1}{2} \qquad (16)$$

3.2 Fitting degree variance models through analytical models

Spherical harmonic degree variances e.g. as computed from 2D-DFT (see previous section) can be approximated by an analytical mathematical function relying on a relatively small number of parameters. These so-called degree variance models are convenient to describe the decay of the gravity signal in general, for estimating the signal power of a gravity functional at a specific spatial scale, and for extrapolating its power to shorter spatial scales. Three selected mathematical models are used to represent computed degree variances in this work, which date back on Kaula (1966), Tscherning and Rapp (1974) and more recently Sanso and Sideris (2013).

The functional model of Kaula's degree variance model is given by

$$c_K^2(l) = \frac{A}{l^B} \quad (= c_l^2[\Psi = 1]) \qquad (17)$$

where $A = 1.6 \cdot 10^{-10}$ (unit: dimensionless) and $B = 3$. The functional model (Eq. 17) is referred to as *Kaula-type* in the following. In brackets the gravity functional to which the mathematical models refers to is given along the lines of the notation in section 2.3.

The original model of Tscherning and Rapp (1974) refers to gravity anomalies and is parameterised as

$$c_{TRorig}^2(l) = \frac{A\,(l-1)}{(l-2)(l+B)} \cdot \sigma_0^{l+2} \left(= c_l^2\left[\Psi = (l-1)^2 \left(\frac{GM \cdot 10^5}{R^2}\right)^2\right]\right) \quad for\ l \geq 3$$

$$c_{TRorig}^2(2) = 7.54\ mGal^2 \qquad (18)$$

$$c_{TRorig}^2(0,1) = 0$$

where $A = 425.28\ mGal^2$, $B = 24$ and $\sigma_0 = 0.999617$ (unit: mGal²). In Sanso and Sideris (2013) the best fitting Tscherning/Rapp model w.r.t. EGM2008 is parameterised as

$$c_{TR_{EGM08}}^2(l) = \frac{A \cdot B^l}{(l-1)(l+2)(l+4)} \quad (= c_l^2[\Psi = 1]) \qquad (19)$$

where $A = 2.8 \cdot 10^{-10}$ (unit: dimensionless) and $B = 0.998365$. Note that this version differs from the original model (Eq. 18). Sanso and Sideris (2013) also present a modified version of their functional model

$$c_{SS}^2(l) = \frac{A \cdot B^l}{(l-1)(l-2)(l+4)(l+17)} \quad (= c_l^2[\Psi = 1]) \qquad (20)$$

in order to better analytically fit the spectrum of the EGM2008 gravity field model. We denote this functional model as *Sanso/Sideris type*. Sanso and Sideris (2013, p158) have published (dimensionless) coefficients $A = 3.9 \cdot 10^{-8}$ and $B = 0.999443$ (ibid, Eq. 3.178) as best fitting analytical description of the EGM2008 spectrum. However, as will be shown in Sect. 4, Sanso and Sideris' numerical values for *A* and *B* are erroneous and do not fit the EGM2008 spectrum well. Instead, Eq. (20) evaluated with $A = 5.0 \cdot 10^{-8}$ and $B = 0.999845$ (derived in this paper with the procedure described next) fits the EGM2008 spectrum in a least squares sense. The functional model in Eq. (20) is well suited to describe spectra of EGM2008 and GGMplus (cf. Sect 4).

Fitting the above models (Eqs. 17, 19 and 20) to computed degree variances is done in an iterative least-squares adjustment approach. During the fit the observations (i.e., the degree variances) are assumed to be without errors, consequently the adjustment yields the same results as a regression (residuals are not used to improve observations).

The gravity signal expressed by degree variances shows a characteristic decrease over several orders of magnitude with increasing spherical harmonic degree, most of it happening in the low degrees. This non-linear behavior would lead to a bias of the fitted curve in the adjustment to the low degrees, where the signal is much larger. In order to overcome this issue the degree variance is substituted by its logarithmic value y:

$$y(l) = \log_{10}(c^2(l)) \; . \tag{21}$$

Another alternative (not further used here) would be to linearize the functional models, e.g., using a Taylor series as proposed by Jekeli (1978).

The partial derivatives $\frac{\partial y}{\partial A}$ and $\frac{\partial y}{\partial B}$ of the three functional models which are needed for the development of the respective design matrix *J* are given in Table 2. When equal and uncorrelated observations $y(l)$ are assumed the weight matrix turns into the identity matrix and the adjustment is given by

$$\Delta\hat{x} = (J'J)^{-1} J'w \tag{22}$$

where $\Delta\hat{x}$=[$\Delta\widehat{A}$ $\Delta\widehat{B}$] is the vector of the adjusted corrections of the initial parameters A_0 and B_0.

Table 2 : Partial derivatives of the functional models (Eqs. 17, 19, 20) by the unknown parameters A and B as needed for the design matrix J

	$\frac{\partial y}{\partial A}$	$\frac{\partial y}{\partial B}$
$y = \log_{10} c_K^2$	$\frac{1}{\ln(10) \cdot A}$	$-\frac{\ln(l)}{\ln(10)}$
$y = \log_{10} c^2{}_{TR\_EGM\_08}$	$\frac{1}{\ln(10) \cdot A}$	$\frac{l}{\ln(10) \cdot B}$
$\mathrm{y} = \log_{10} c_{SS}^2$	$\frac{1}{\ln(10) \cdot A}$	$\frac{l}{\ln(10) \cdot B}$

The vector w describes the disagreement between observations and the function evaluated with the initial parameters

$$w = y(l) - \log_{10}(c^2(l, A_0, B_0)). \quad (23)$$

Then the adjusted parameters are

$$\hat{A} = A_0 + \Delta\hat{A} \quad (24)$$

$$\hat{B} = B_0 + \Delta\hat{B}\,. \quad (25)$$

The iterative process is terminated when $\Delta\hat{A} < 10^{-13}$ and $\Delta\hat{B} < 10^{-8}$ (for Kaula-type models $\Delta\hat{B} < 10^{-5}$). Using these criteria four to five iterations are found to be necessary for the fit (up to ten for Kaula-type models), depending on the choice of the initial parameters.

3.3 Empirical investigation of the 2D-DFT approach

3.3.1 Effects of class width, averaging, regional coverage and evaluation height

In the literature, the 2D-DFT approach described above (section 3.1) has been applied on local or regional data sets. The application of the method with global scope needs further investigation. We focus on determining the approximation errors by comparisons between 2D-DFT-recovered spectra from dV-SPH-RET2012-derived gravity against those directly from the dV-SPH-RET2012 SHCs which serve as true reference. This allows us to test the influence of free parameters in the 2D-DFT (e.g., class width) in a closed-loop environment.

Of particular interest is the effect of a tiling of the input gravity grids on the spectra in view of an application of the 2D-DFT for computing degree variances from GGMplus (see section 4.1). It provides gravity at the surface of the topography only over the continental landmasses of the Earth (except for polar regions). We therefore compare the global spectra recovered from regional averages with spectra recovered from one global grid processed at once, study the effect of the data extent and investigate the role of the evaluation height in the synthesis of dV-SPH-RET2012 gravity on the degree variances spectra. Next we test a range of simple scenarios based on the global 5 arc-min grid of dV-SPH-RET2012 gravity disturbances (Fig. 1, Eq. 4) as input for the 2D-DFT.

- Processing a global grid

  In this test, we apply the 2D-DFT on the global dV-SPH-RET2012 gravity disturbance grid without any tiling. The mean latitude of the global grid is zero and $\mathrm{D_x}$ and Dy become 40075.0 km and 20035.5 km, respectively. The recovered degree variances (Fig. 4a) show greatest deviations from the original degree variances (black line) for the very low (< 40) and very high degrees (>2000), see detail plots in Fig. 4b and Fig. 4c. In the low frequencies the deviations are directly related to the azimuth averaging and the chosen class width, e.g. $\Delta h = 50$ (cyan line), which in this case indicates that the computed degree variance values are actually averages over +/-25 spherical harmonic degrees of the denoted degree. Thus, the parameter Δh (see section 3.1) defines the spectral resolution of the 2D-DFT

approach and $\Delta h = 20$ seems to be a good compromise in terms of smoothness and spectral resolution. As the signal decay is very steep (and exponential) near the low-degree harmonics, the averaged values are rather overestimates.

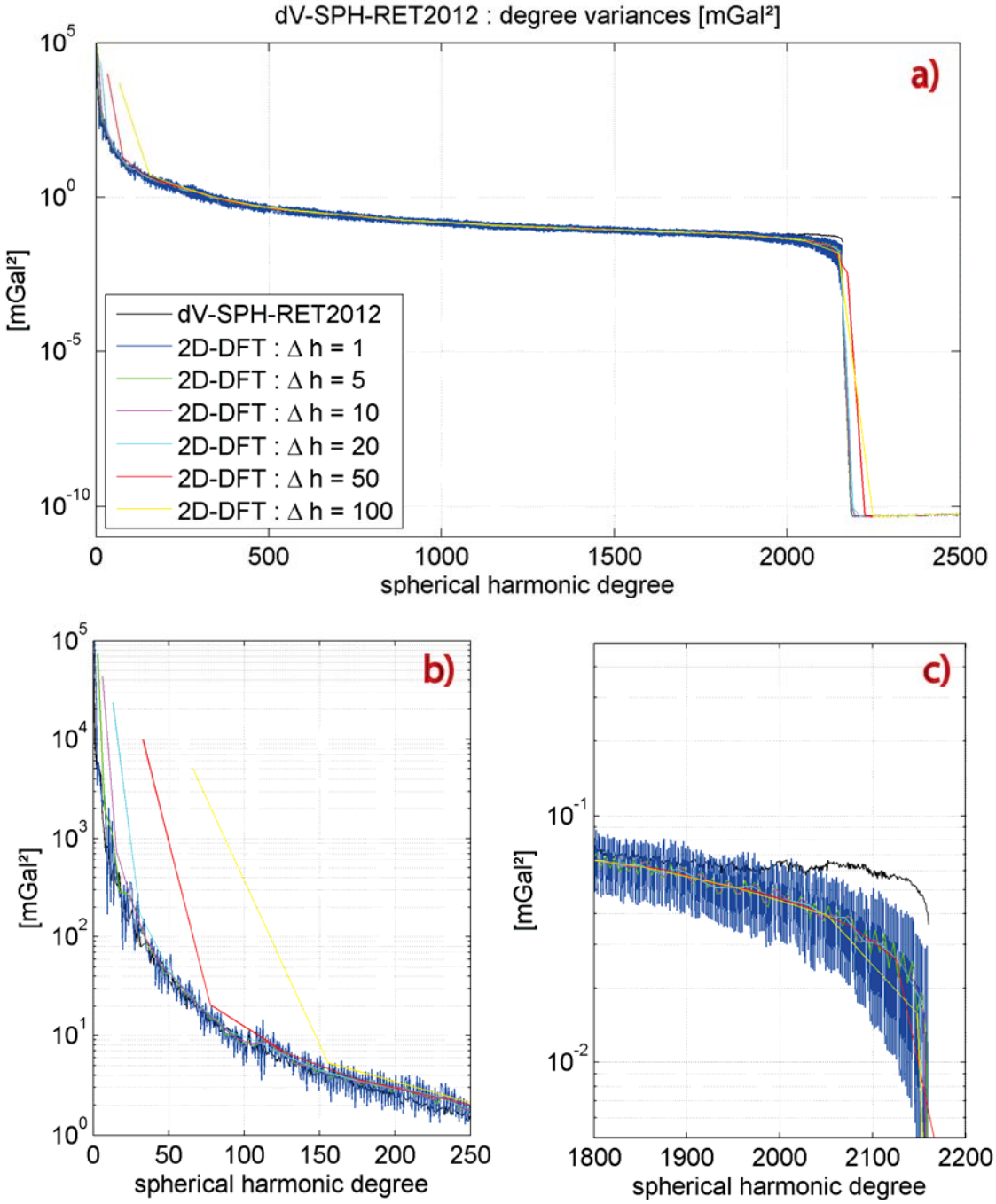

Figure 4: Degree variances from original topographic potential model dV_SPH_RET2012 (in black) and the degree variances retrieved by 2D-DFT (coloured lines) for various different class-widths Δh (in degrees), degree variances are in in mGal^2.

In the very high frequencies, the signal is underestimated as the recovered degree variances dip away beyond degree ~2000 (Fig. 4c). The behavior in the high degrees is related to the chosen gravity grid sampling of 5 arc-min, which is near the Nyquist frequency for high harmonic degrees (the high frequencies near degree 2160 are not well represented at 5 arc-min resolution). By increasing the grid sampling to 1 arc-min

(oversampling of factor 5) in the synthesis, the signal power beyond 2000 can be retrieved with almost the same quality as for degrees < 2000 (not shown here). The recovered degree variances correctly drop by about eight orders of magnitude around degree 2160, which is the resolution of the input model.

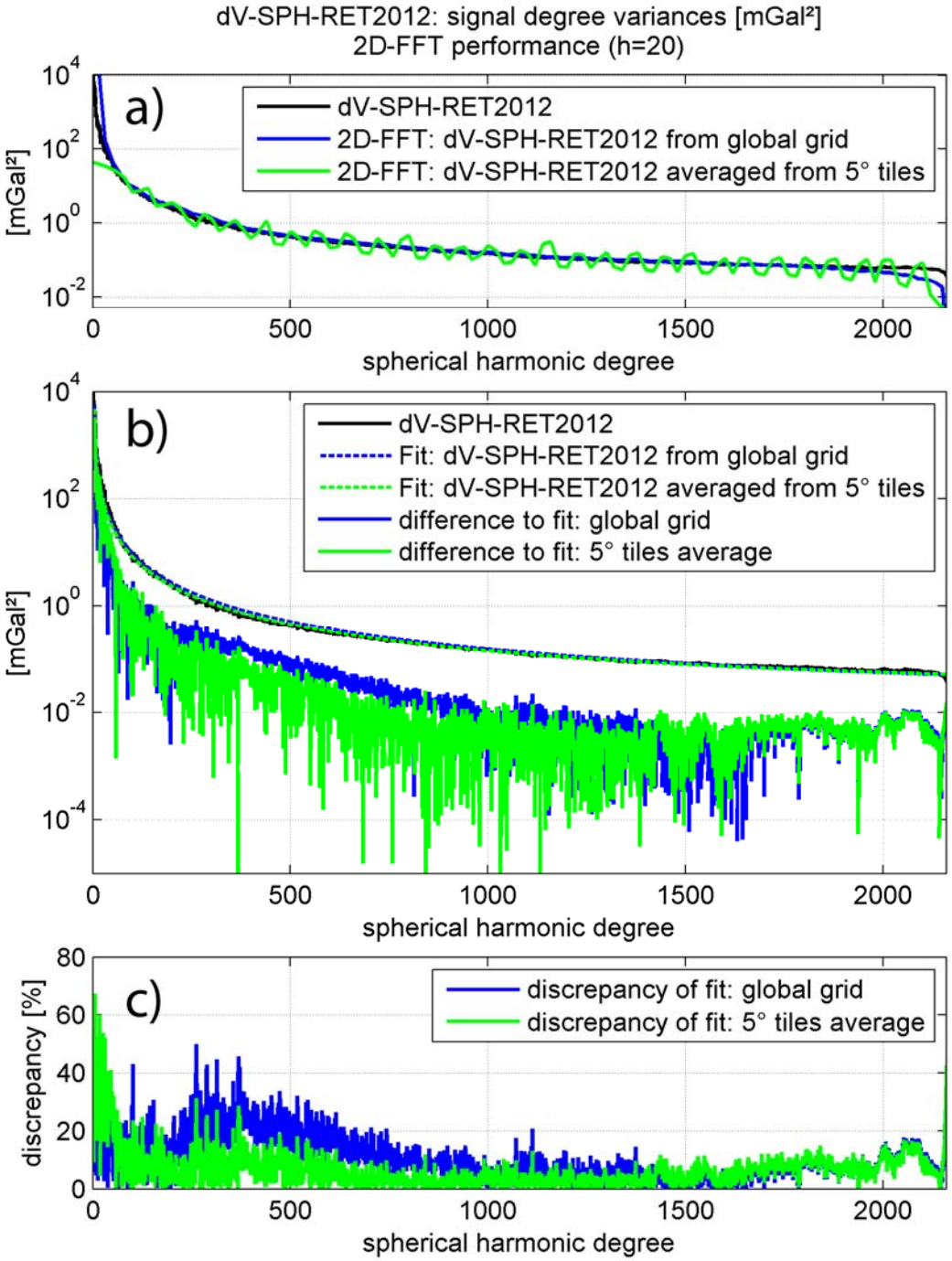

Figure 5: Closed-loop performance of 2D-DFT approach based on the topographic potential model dV-SPH-RET2012 when applied on global grid (blue lines) and on 5°x5° tiles with consecutive averaging (green lines) in terms of gravity disturbances [mGal²]

- Role of tiling and averaging

In a second step, the global grid of synthesised gravity disturbances is divided into 2592 5° x 5° tiles and each of the tiles is evaluated by the 2D-DFT approach. The average of the 2592 computed degree variances (Fig. 5a, green line) oscillates around the true degree variances (black line). For comparison purposes, the 2D-DFT recovered spectrum of the global dV_SPH_RET2012 gravity grid are shown too (Fig. 5a, blue line), revealing there are no notable oscillations. The amplitude and frequency of the oscillations associated with the tiling are to some extent related to the tile size (decreasing the tile size leads to a lower frequency but a higher amplitude and vice versa). The ability for retrieval of the low-degree harmonics is limited because the maximum wavelength in a 5° x 5° tile is ~ 555 km. Therefore the spherical harmonic degrees below ~ 36 cannot be recovered, which explains why the low-frequency power cannot be retrieved in the same manner as the 2D-DFT applied to a global grid. However, this effect is non-critical for this study because of our interest in the GGMplus gravity field spectra at short scales.

Fitting a Sanso/Sideris-type model (Eq. 20) to the averaged degree variances between degree 50 … 2000 (Fig. 5b, dashed green line for spectra from tiled data, dashed blue line for grid processed as whole), the differences with respect to the true dV-SPH-RET2012 SHC-derived spectrum are at the 10 % level and hardly exceed 20 % (Fig. 5c).

In summary, the fairly good agreement in the closed loop tests show that the 2D-DFT method is capable of recovering the gravity power spectra with reasonable quality. There are ~10% errors over much of the spectrum when using regional tiles. The choice of the tile size puts limitations to the minimum recoverable degree and the tiling and averaging leads to an oscillation of the signal around the original degree variance. Most importantly, the oscillations do not deteriorate the fit, and the precision of the tiling and averaging procedure is commensurate or even better compared to processing a global grid at once.

- Role of coverage

In view of spectrally analysing GGMplus gravity maps, available only for land areas in between 60° North and 56° South, the effect of different global coverage on the spectra is important. Therefore, the dV-SPH-RET2012 gravity disturbance grid is divided into 10° x 10° tiles and degree variance averages for selected spatial coverages are computed and analysed. The fitted degree variance curves in Fig. 6 indicate the following: polar regions contain less topographic gravity signal over nearly all scales, because excluding tiles North of 60° and South of -60° latitude from the average (red line) leads to more power in the degree variances than the global grid (dark blue line); additionally excluding all tiles entirely located over the oceans (green line) leads to even more power in the degree variances; hence, the continental areas are covered by higher-power topographic gravity features compared to the bottom of the oceans. Conversely, averaging only the degree variances from ocean tiles (light blue line) leads to signal power below the global energy level in the spherical harmonic domain. Note that these considerations hold for the topographic potential (and probably for gravity at very short scales), but not necessarily for Earth's actual gravity field.

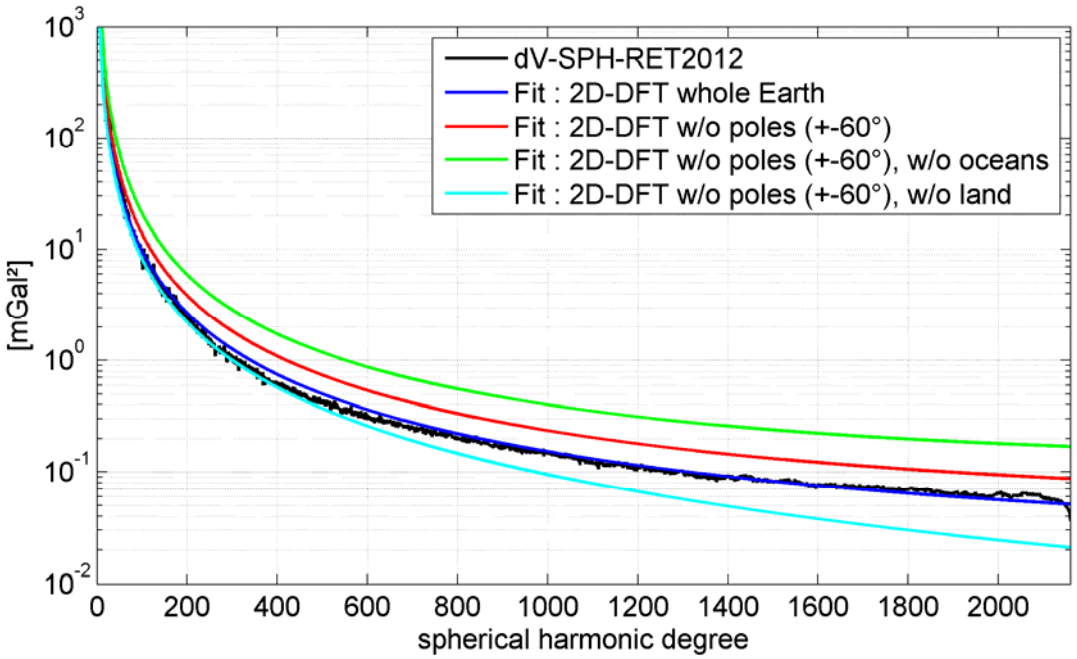

Figure 6: 2D-DFT signal degree variance fits from synthesised dV-SPH-RET2012 gravity disturbance grid in dependence of different global coverage

- Role of evaluation height

In the experiments above gravity values were synthesised on the sphere (r=R). In geodetic practice, gravity is often given on the surface of the topography (e.g. measurements or gravity models such as GGMplus). In spherical approximation, evaluation at the surface of the topography is done by introducing r=R+H in Eq. 4. Gravity signals at the reference surface (e.g. sphere) are downward-continued and thus amplified compared to signals at the surface of the topography. In Fig. 7 the 2D-DFT procedure has been applied to a global grid of gravity disturbances of the spherical topographic potential model dV-SPH-RET2012

- evaluated at the surface of the model's reference sphere (light blue line) and
- evaluated at the surface of the topography (red line) using an upward continuation technique along with gravity gradients of up to sixth order (see Hirt 2012 for details).

For comparison purposes, the true dV-SPH-RET2012 degree variances computed from SHCs are shown as well (dark blue line). The degree variance curves start to deviate near degree 600 where the red degree variances fall below the energy level of degree variances at the sphere. At degree 2000 the difference between the "topography-residing" and the "sphere-residing" degree variances reaches a factor of ~2.8.

This behavior is explained by the attenuation of gravity with height. At the reference sphere gravity (e.g. gravity disturbances) is downward continued, thus amplified. With increasing height gravity becomes attenuated. This particularly affects short scale signals because the attenuation effect becomes stronger the shorter the associated wavelengths. From Fig. 7, it is thus important to discriminate between spectra of gravity provided at the reference sphere, and those at the surface of the topography.

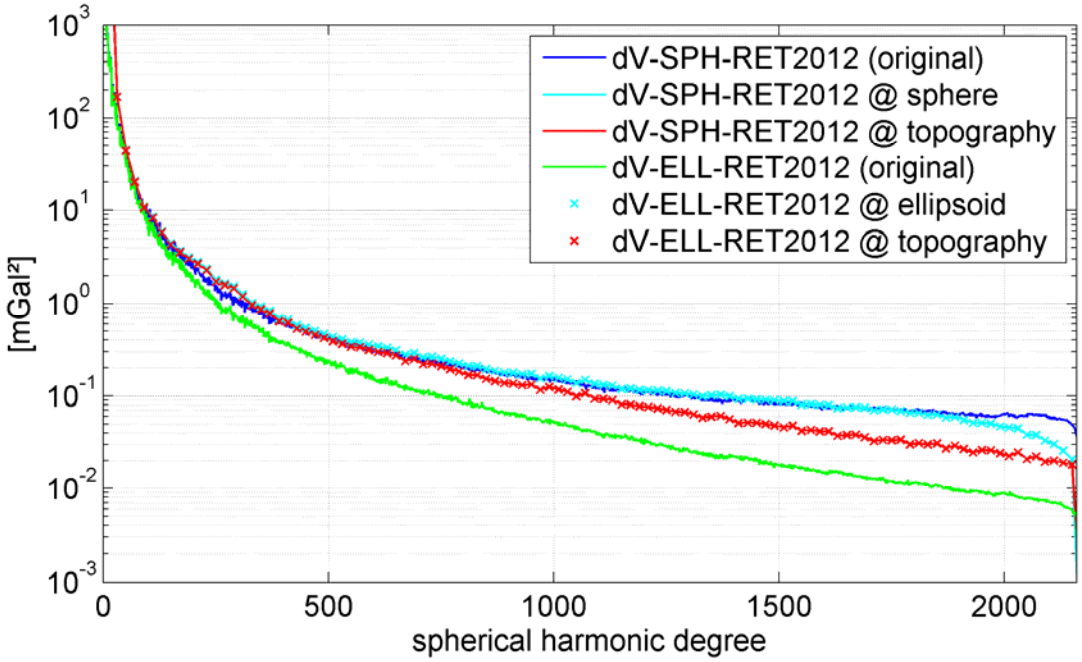

Figure 7: Results of 2D-DFT experiments using two different models evaluated on different surfaces such as sphere, ellipsoid and topography: 1) topographic potential model dV-SPH-RET2012 (from SHCs, blue line), and 2D-DFT-recovered spectrum from gravity disturbances evaluated at the sphere (cyan line), at the topography (red line), at the topography (fit) over 5°x5° land tiles (no oceans) within +- 60° latitude (magenta line); 2) topographic potential model dV-ELL-RET2012 (green line) recovered from gravity disturbances evaluated at the ellipsoid (cyan cross), at the topography (red cross); unit in mGal².

3.3.2 Degree variances in ellipsoidal and spherical approximation

To study the effect of ellipsoidal approximation (see chapter 2.2 for the definition in our context) in the 2D-DFT technique, we have synthesised gravity from the ellipsoidal topographic potential model dV-ELL-RET2012 (which is the "counterpart" to the spherical topographic model dV-SPH-RET2012) and investigated the (2D-DFT) recovered spectra. The original degree variance spectra of dV-ELL-RET2012 (green line) and dV-SPH_RET2012 (blue line) already differ, and the decay of the ellipsoidal approximated spectra (green) is stronger than the spherical approximated spectra (blue) with increasing degree (Fig. 7.). This is due to different attenuation factors ($(a/R)^{l+1}$ $vs.(a/r_e)^{l+1}$) that are implicitly contained in the spherical harmonic coefficients (c.f. Claessens and Hirt 2013). In Fig. 7 the 2D-DFT technique has been applied to a global grid of dV-ELL-RET2012 gravity disturbances

- evaluated on the surface of the model's reference ellipsoid (light blue crosses); $r = r_e$ (see Eq. 4); and
- evaluated at the surface of the topography using the gradient continuation technique as above (red crosses); $r = r_e + H$ (see Eq. 4) .

Importantly, the recovered spectra of dV-ELL-RET2012 (light blue/red crosses, Fig. 7) almost exactly follow the recovered spectra of dV-SPH-RET2012 (light blue /red line) (see last paragraph of previous subsection). This is due to the spherical nature of the 2D-DFT approach, given by applying a constant radius R in Eq. 13. Hence, the 2D-DFT refers to a truly spherically

approximated Earth and cannot be used to recover degree variances in ellipsoidal approximation. When applying the 2D-DFT approach to a grid of gravity disturbances from the ellipsoidal topographic potential model dV-ELL-RET2012 (2 … 2190), we obtain degree variances which are (quasi) transformed/compatible to their spherical counterpart (dV-SPH-RET2012).

The distinctly different decay between spherical and ellipsoidal approximation can be expressed by the ratio $\frac{c_l(dV\_ELL\_RET2012)}{c_l(dV\_SPH\_RET2012)}$(black line, Fig. 8). For the very low degrees the approximations nearly coincide while the gap becomes larger (non-linearly) towards the high degrees, where the spectra differ in the order of 10^{-1} at degree 2160.

Describing this ratio $\alpha_l^{e/s}$ by a 1st order polynomial (as exponent to 10) as a function of the degree l with $k_0 = -4.5511 \cdot 10^{-2}$ and $k_1 = -4.1104 \cdot 10^{-4}$ following

$$\frac{c_l(dV\_ELL\_RET2012)}{c_l(dV\_SPH\_RET2012)} \sim \alpha_l^{e/s} = 10^{(k_0 + l \cdot k_1)}, \qquad (26)$$

yields quite a good fit for degrees larger than 150 (see red line, Fig. 8). In Eq. (26) the superscripts e/s indicate it is a ratio between degree variances of ellipsoidal and spherical approximation. In approximation the ratio $\alpha_l^{e/s}$ can now be used as an empirically derived rule of thumb for a transformation of degree variances of any degree l>150 from spherical to ellipsoidal approximation of the underlying mass distribution, and vice versa.

Note that the empirical law is derived from degree variances of the topographic potential, and therefore it is primarily applicable to any functional derived from this topographic potential. As the dimensioning factor Ψ in Eq. 3 cancels out in the ratio, the rule is valid for any gravity functional. As an aside, fitting an 8th order polynomial to the ratio yields a very good fit for degrees l<150 (see green line, Fig. 8), however, eight parameters are not considered very handy for a rule of thumb.

The rule of thumb applied to both RET2012 topographic potential models (Fig. 9) show an average disagreement of 2.1 % (over all degrees) to the respective other model, with discrepancies per degree hardly exceeding 10 %. The rule of thumb allows generation of a spherically approximated spectrum of EGM2008 (or any other potential model) at degree variance level (grey line, Fig. 9), which closely follows the spherically approximated model dV-SPH-RET2012 (for degrees > ~250).

Besides, Fig. 9 shows that the spectrum of the Earth Gravitational Model 2008 model (black line) can be directly compared with that of the dV-ELL-RET2012 model. The very close agreement over most part of the spectrum demonstrates that EGM2008 is in ellipsoidal approximation (as expected).

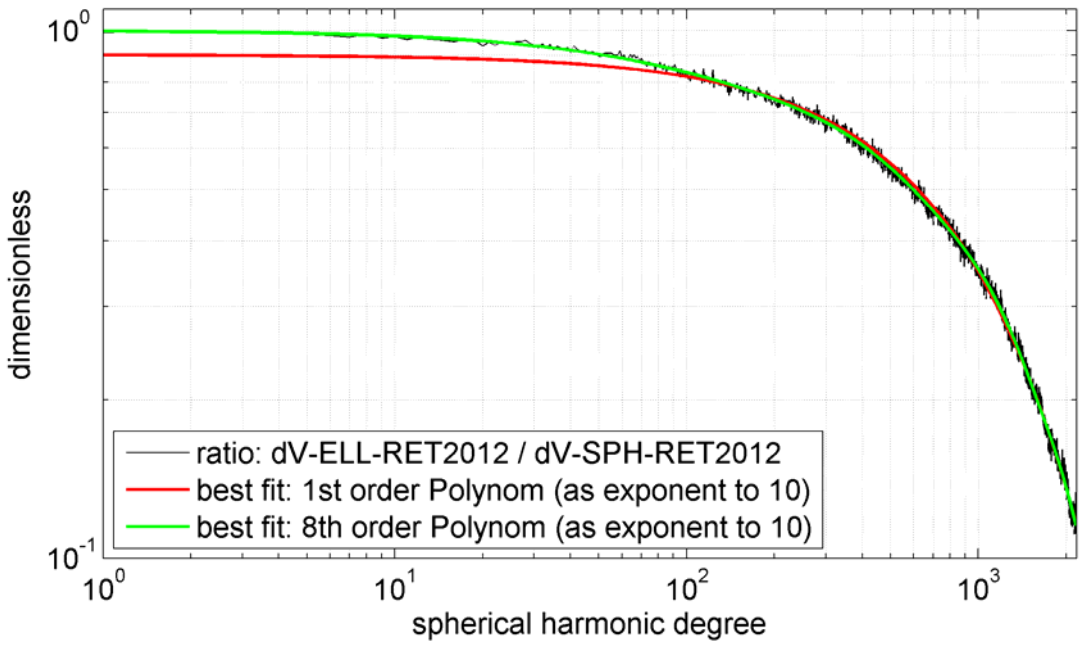

Figure 8: Ratio between the spherically and the ellipsoidally approximated degree variances of the topographic potential [dimensionless]

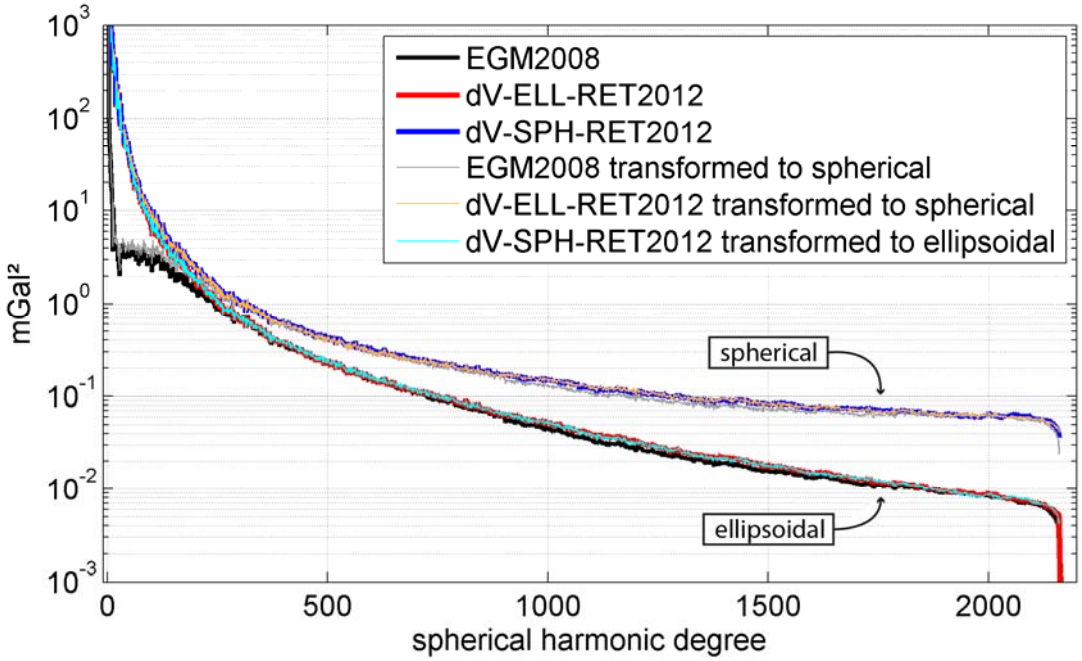

Figure 9: Transformation of the degree variances of three selected spherical harmonic models between their ellipsoidal and their spherical approximation using the rule of thumb (equation 26)

3.3.3 Discussion

The above experiments investigating the 2D-DFT approach provide valuable insight into the interpretation of degree variances of the spherical harmonic series and the applicability of the 2D-DFT approach for recovery of these spectra.

In general, the experiments show that due care is needed in the interpretation of degree variances obtained from gravity values measured / synthesised on the topography. At the

reference surface (r=R) the gravity is amplified (for all functionals), e.g. gravity disturbances according to $(\frac{R}{r})^{l+2}$. Therefore the 2D-DFT spectra generated from gravity at the topography (r>R) exhibit less energy than those retrieved directly from the original spherical harmonic models that refer to the underlying reference body, especially in the high degrees (beyond degree 600). In order to be consistent, the gravity values would have to be downward continued to the reference body of the geopotential model before applying the 2D-DFT procedure.

Additionally, the type of approximation chosen for the underlying mass distribution of a topography-implied SH model, i.e. spherical or ellipsoidal approximation, yields different energy levels in the spectrum according to an attenuation factor, that is implicitly contained in the spherical harmonic coefficients. The spherical approximation, historically and even today, often plays an important role in forward modelling Newtonian gravity from the topographic masses (Balmino et al. 2012; Hirt and Kuhn 2014).

With the new empirical rule of thumb (Eq. 26), derived from two topographic potential spectra, one can transform the degree variance between its spherical and ellipsoidal representation (Fig. 9). The method is only approximate (~ 10 %) and derived from topographic potential models, thus it may yield larger discrepancies for geopotential models, especially at low-degree harmonics. Furthermore, the transformation applies in degree variance domain and is a good approximation at least for the degrees 150 to 2160.

The comparison of the degree variances shows that the spectral power of the ellipsoidal models is (seemingly) smaller than of the models in spherical approximation, and this effect becomes more pronounced as the harmonic degree increases (Fig. 7, particularly Fig. 9). This behavior of the degree variances reflects that the mass distribution in spherical approximation is close to the reference radius, while being up to ~20 km below the reference radius (at the poles) in ellipsoidal approximation. Because of the radial dampening of the field, the amplitudes of the degree variances are thus much lower in ellipsoidal approximation. This is both the case for EGM2008 and the topographic potential model dV_ELL_RET2012, both reflecting ellipsoidal mass distributions. The lower spectral energy associated with the ellipsoidal models (Fig. 9) does not represent a smoother gravity field, but rather the [ellipsoidal] location of field-generating masses w.r.t. to the reference radius of the spherical harmonic model.

Balmino et al. (2012) noted different energy levels between their topographic potential and the EGM2008 geopotential model at short spatial scales, down to degree 2160 (ibid, see Figure 10). The authors find the spectral energy of the topographic potential to be “significantly larger” and attribute this to a “well known sign of a compensation mechanism such as isostasy”. However, our results show that the differences simply reflect two levels of approximation: While EGM2008 is in ellipsoidal approximation, their generated topographic potential coefficients are in spherical approximation as they reflect the topographic masses arranged on the surface of a sphere. Our work, especially the developed rule for the transformation between the two approximations (ellipsoid vs. sphere), can thus be seen as an extension to their work. We expect the developed rule to make their power spectrum more compatible to models in ellipsoidal approximation, such as EGM2008.

The 2D-DFT approach is capable of delivering spherically approximated spectra only. This is because it relies on the transformation of Forsberg (1984a), which uses a constant (mean) Earth radius (Eq. 13). Applying the 2D-DFT globally for recovery of gravity spectra yields pleasingly good results given the simplicity of the approach and taking into account that some 2D-DFT prerequisites are being violated (e.g. equidistant spacing, periodicity). This even holds true for working in small tiles and consecutive averaging over the spectra of all tiles. With the tiling procedure, the degree variances of a potential model can be retrieved from a global grid with discrepancies at the 10-20 % level over large parts of the spectrum by fitting an appropriate degree variance model to it. This is considered sufficient for the derivation of gravity power spectra. The tiling allows for the evaluation of degree variances in selected regions of the Earth, e.g. the spectral energy over polar regions, continental landmasses, the oceans or areas of different terrain type. The method is therefore suited for estimation of high-degree spherically approximated degree variances from GGMplus gravity grids (next Section).

4. Approximation of the Earth's gravitational potential energy to ultra-short spatial scales

4.1 Data and Processing

In this section information on the data and the workflow for an approximation of the power spectrum of the topographic potential as implied by the Earth's land topographic masses in terms of degree variances for the degrees 2160 up to 90000 by 2D-DFT are provided.

For this purpose we make use of the GGMplus (Hirt et al. 2013) gravity maps. GGMplus is a set of digital gravity maps available for different gravity functionals with near-global coverage (all landmasses from -56° to 60° latitude). The gravity implied in the maps is a combination of satellite gravity, gravity as given by EGM2008 (Pavlis et al. 2012) and forward modelled topographic gravity up to ultra-short scale. In the low to mid-range frequencies (degrees 0 … ~180) the maps rely on a combination of ITG-GRACE (Mayer-Gürr et al. 2010) and GOCE (Pail et al. 2010) satellite information (equivalent to GOCE-TIM4 release). Gravity information from EGM2008 (Pavlis et al. 2012) supersedes the satellite-only information in the maps near degree 190. EGM2008 is dominant in the degrees 200 … 2190. From degree 2160 up to degree ~90,000, corresponding to spatial scales ranging from ~10 km down to ~220 m, the maps rely on forward modelled topographic gravity. The forward modelling is achieved assuming a standard rock-density of 2670 kg/m³ and applying residual terrain modelling (RTM) procedures (Forsberg 1984b) based (mainly) on topographic information of the Shuttle Radar Topography Mission (SRTM) (Farr et al. 2007). More information on the computation of the GGMplus maps can be found in Hirt et al. (2013). The maps can be accessed at http://ddfe.curtin.edu.au/models/GGMplus/.

We have chosen GGMplus maps of gravity disturbances (radial derivative of the disturbing potential) which provide the anomalous part of the gravity acceleration with a formal resolution of 0.1 microGal ($1\,\mu Gal = 10^{-8}\,\frac{m}{s^2}$) for the evaluation with the 2D-DFT. In principal, other functionals, e.g. quasi-geoid heights, could be used likewise for the evaluation. However, topographic gravity signals at scales of 250 m might not be represented fully by the provided data resolution of 1 mm for quasi-geoid heights.

The maps come in 5° x 5° sized tiles with an equi-angular grid sampling of 7.2 arc-seconds. Inserting the tile size in Eq. 15 and the sampling in Eq. 16, yields a minimum and maximum retrievable degree of ~ 36 and ~90000, respectively. Hence, both the 2D-DFT method and the data allow the approximation of power spectra of the topographic potential between degree 2160 and ~ 90000.

The processing of the GGMplus tiles exactly follows the procedure of our closed loop test performed with tiles of the topographic potential model dV-SPH-RET2012 (section 3.1), except for the tile size which is decreased to 2.5°. The smaller tile size allows finer selection of ocean and non-ocean tiles, thus takes into account more gravity data closer to the shore line, extending the landmasses covered by our analyses (see Fig. 10). The degree variances are computed for each single 2.5° x 2.5° inland tile and then all tiles are averaged to obtain an approximation of the topographic potential degree variances over the landmasses of the Earth.

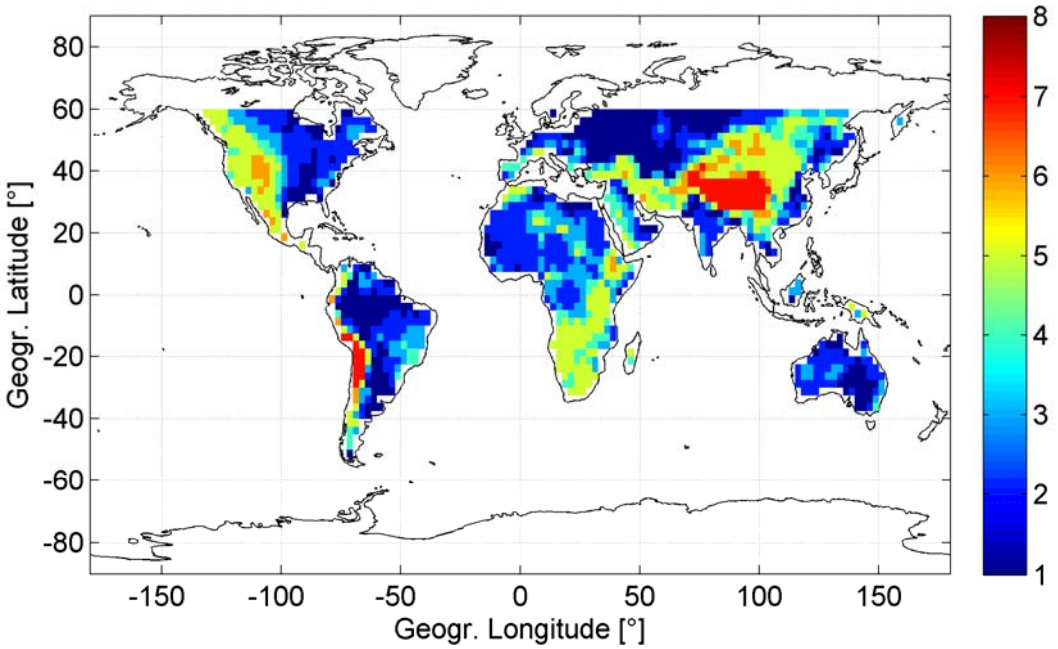

Figure 10 : Global coverage with utilized GGMplus 2.5° x 2.5° tiles and their classification into seven terrain RMS classes

As a refinement, this is also done for different types of terrain: from low elevated to high elevated terrain. The terrain type is determined by means of the root-mean-square (RMS) over the heights in each tile. We will refer to this indicator as *Terrain RMS* in the following. The colour of the degree variances is linked to the class colour attributed to each class in Fig. 10, that visualises the spatial distribution of the tiles by *Terrain RMS*. Seven groups of terrain roughness are defined given by the following thresholds for the *Terrain RMS*: 0- 250 m (1), 250 – 500 m (2), 500 – 750 m (3), 750 – 1000 m (4), 1000 – 2000 m (5), 2000 – 3000 m (6), > 3000 m (7). The latter class contains parts of the Andes and Himalaya mountains as highest elevated areas of Earth.

Any tile containing non-available numbers (i.e., cells 10 km or more apart from the coast line) is excluded from the computation, as gravity is not provided offshore in GGMplus.

Alternatively, (i) ocean tiles could have been filled with zeros which would underestimate the spectral power, or (ii) marine gravity from altimetry could be filled in, which however does not resolve the field much below 4 arc-min scales.

Our derived degree variance models are based on the functional model of the Sanso/Sideris-type model (Eq. 20), with the coefficients *A* and *B* estimated using our least-squares fitting procedure (section 3.2). This model has been identified to approximate the computed degree variances best, based on the least-square fit residuals. The computed degree variances of the topographic potential are an approximation of the Earth's actual geopotential spectra due to several reasons:

- the forward modelling in GGMplus uses uniform rock-density; the actual gravitational attraction caused by the topographic masses might therefore be over- or underestimated in some places.

- the topographic heights used in the forward modelling are from the SRTM model which is not free of errors (see, e.g. Rexer and Hirt (2014)).

- approximation errors of the 2D-DFT method for the computation of degree variances with respect to rigorous spherical harmonic modelling (about 10 – 20 % in terms of degree variances, see Section 3, Fig. 5).

- non-global coverage; GGMplus is limited to the landmasses in between -56° to 60° latitude while degree variances of the spherical harmonic representation are per se defined in a truly global sense.

We note that GGMplus gravity values and thus also the derived spectra represent the gravity at the Earth's surface (on top of the topography), and not at some reference body (ellipsoid or sphere).

4.2 Results

4.2.1 Degree variances and models

In this section degree variances estimated from GGMplus gravity maps are presented following the procedures described above.

The black curve in Fig. 11a illustrates the average degree variance of all 1502 2.5° x 2.5° tiles. The signal of all averages shows (i) the decay of the signal with rising degree and (ii) strong oscillations towards the ultra-high frequencies. The oscillations stem from the tiling of the global grid in 2.5° tiles (c.f. Sect. 3). As explained above, the oscillations are of lower frequency and of higher amplitude the smaller the tiles are. The oscillations showed not to have negative impact on the fit. The coloured degree variance curves in Fig. 11a reflect the average degree variances in our seven different classes of terrain. With this classification we can give estimates for the gravitational power of the topographic masses on small scales as a function of the terrain's elevation. The variances confirm that the higher the Terrain RMS (meaning: the larger the amount of the topographic masses) the higher the gravitational signal (meaning: higher variability of attraction). In addition, by grouping the tiles by the STD of the elevation instead of by RMS, we may say that the rougher the terrain (meaning: the more mountainous)

the higher the gravitational signal, and the flatter the terrain the lower the gravitational signal (results not shown here in detail).

Fitting curves to the computed degree variances using the functional model of the Sanso/Sideris-type degree variance model (Eq. 20) yields the curves in Fig. 11b, with the (individual) model coefficients *A* and *B* reported in Table 3. Note that the values in the degree range 0…2160 are extrapolations for the seven terrain class models, as the models are fitted from computed degree variances starting at degree 2160. The degrees below 2160 were neglected, because the focus of this study lies upon the very high frequencies and including the lower degrees leads to a poorer fit in the upper part of the spectrum.

The fitted curves provide a clearer picture of the signal power at all scales. As expected, the average over all tiles (black curve) is found in the middle of the other curves, close to the equivalent of tiles with Terrain RMS of around 750 m.

4.2.2 Omission errors from computed degree variance models

Omission errors in physical geodesy denote the error associated with the truncation of the infinite series (of spherical harmonic functions) at some maximum degree. Degree variances calculated from degree variance models may easily be transformed into omission errors. The error ε_{OM} is defined as the sum over all squared spherical harmonic coefficients CS_{lm}^2 of degree $l > l_{max}$ and thus may be written as

$$\varepsilon_{OM} = \sum_{l=l_{max+1}}^{\infty} \sum_{m=-l}^{l} CS_{lm}^2 = \sum_{l=l_{max+1}}^{\infty} c_l^2 \ . \qquad (27)$$

In Table 4 the omission errors for three different truncation degrees ($l_{max} = 2160, 10800, 21600$) of popular degree variance models and of degree variance models computed from the different GGMplus spectra are listed. The omission error here is evaluated up to degree 90000 (and not up to infinity) in terms of gravity disturbances and geoid heights.

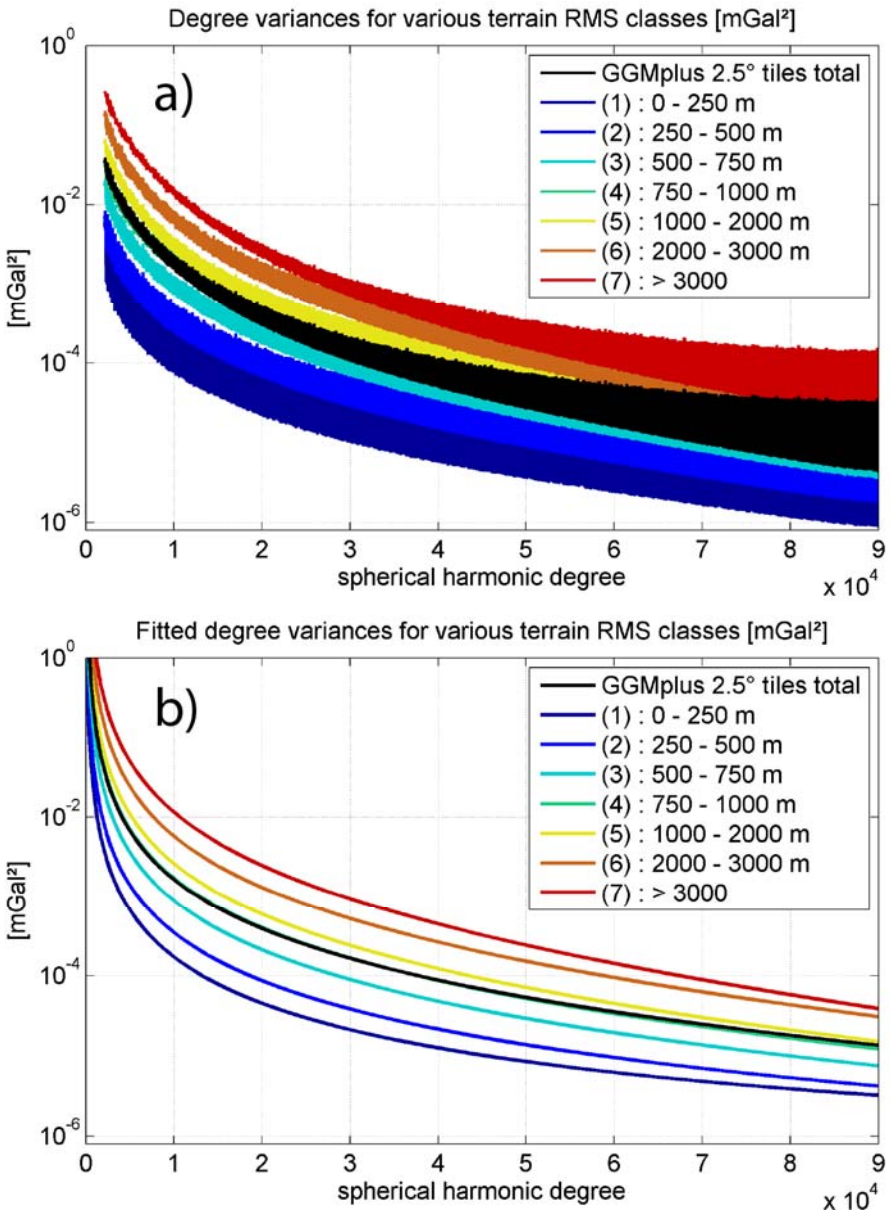

Figure 11 : Resulting GGMplus degree variances (total average : black line); a) Class averages of the degree variances computed in each tile by 2D-DFT; b) Fitted degree variance curves for each class by means of a best fitting Sanso/Sideris-type model (Eq. 20)

4.2.3 Interpretation and discussion of results

When comparing our degree variances to the spherical harmonic spectra of global geopotential models (or common degree variance models), we keep in mind that

(a) for degrees higher than 2160, the computed degree variances reflect only the gravitational signal implied by the topographic masses,

(b) our degree variances are not truly global (although presented in spherical harmonic domain) and

(c) the degree variances represent gravity on top of the topography and not directly at any reference surface (e.g. a sphere or an ellipsoid). This makes our degree variances "incompatible" to those from global spherical harmonic models, which represent

gravity downward-continued to some reference surface. Downward-continuation of the GGMplus gravity with procedures described in Pavlis et al. (2012) would make the spectra more mutually compatible, however this remains as a future task.

It was shown in subsection 3.3.1 that (b) leads to an overestimation (as poles and oceans are excluded) and (c) to an underestimation of the power spectrum. Our calculated degree variances contain a mixture of both effects. This in turn suggests how the presented degree variances (models) are to be interpreted and used: they reflect the signal of the topography-implied gravity field over the continental landmasses, as sensed directly at its surface (the topography). Due to the generation procedure our degree variances are close to spherical approximations of the topographic potential, i.e. the underlying reference surface is a sphere (see Fig. 7).

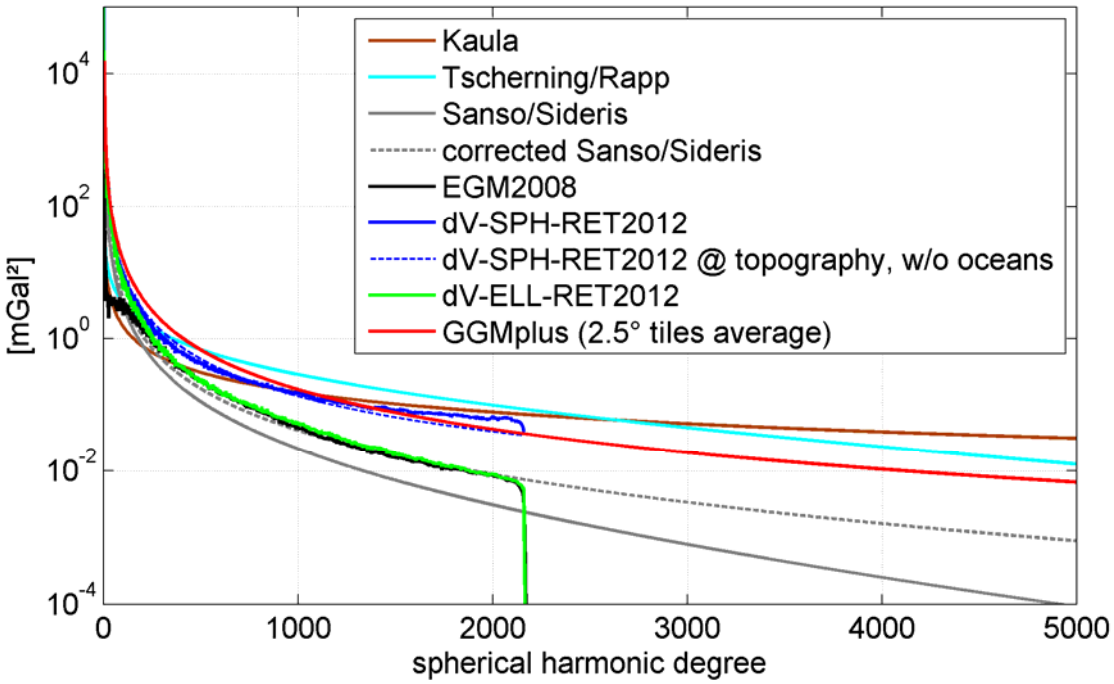

Figure 12: Overview on computed GGMplus degree variances and selected well-known degree variances (from models) in terms of gravity disturbances [mGal²]; for degrees 0...5000

As the central result of our study Fig. 12 shows the fitted GGMplus-based degree variances (solid red line) together with spectra of other selected degree variance models (Kaula, Tscherning/Rapp, Sanso/Sideris), and directly computed spectra from the spherical harmonic model coefficients (EGM2008, and of topographic potential models dV-SPH-RET2012 and dV-ELL-RET2012). For comparison purposes, the 2D-DFT recovered spectra from dV-SPH-RET2012 gravity (evaluated at the topography, over continental 5° x 5° sized tiles within +- 60° latitude only, which is comparable to the GGMplus data area) is shown (dashed blue line). From Fig. 12, the models clearly group into ellipsoidal approximation (EGM2008, dV-ELL-RET2012, Sanso/Sideris) and spherical approximation (dV_SPH_RET2012, Kaula, Tscherning/Rapp). The latter sets of degree variances have somewhat more power than those evaluated at the topography (GGMplus and dV-SPH-RET2012 at the topography).

Table 3 : Coefficients A and B of Sanso/Sideris-type degree variance models (equation 20) as estimated for different spherical harmonic potential models and for GGMplus gravity tiles via 2D-FFT. The degree variances c_l^2 received when evaluated with equation 20 are dimensionless ($\Psi = 1$).

Source of degree variances	***valid for degrees***	***number of tiles used***	***SS-type model***	***A***	***B***
Sanso & Sideris (2013) – EGM2008	0 … 2160	-	original	3.9e-8	0.999443
EGM2008 @ ellipsoid (corrected Sanso & Sideris model)	3…2160	-	this work	5.0e-8	0.999845
dV_ELL_RET2012 @ ellipsoid	3…2160	-	this work	8.69e-8	0.999528
dV_SPH_RET2012 @ sphere	3…2160	-	this work	9.65e-8	1.000475
GGMP Tr 2.5° - all land tiles @ topography	4 … 90000	1502	this work	1.79e-7	0.999995
GGMP Tr 2.5° - only land : Terrain RMS 1	2160 …90000	330	this work	1.69e-8	1.0000053
GGMP Tr 2.5° - only land : Terrain RMS 2	2160 …90000	408	this work	3.62e-8	0.9999997
GGMP Tr 2.5° - only land : Terrain RMS 3	2160 …90000	221	this work	9.62e-8	0.9999953
GGMP Tr 2.5° - only land : Terrain RMS 4	2160 …90000	143	this work	1.91e-7	0.9999931
GGMP Tr 2.5° - only land : Terrain RMS 5	2160 …90000	291	this work	2.98e-7	0.9999905
GGMP Tr 2.5° - only land : Terrain RMS 6	2160 …90000	49	this work	6.67e-7	0.9999895
GGMP Tr 2.5° - only land : Terrain RMS 7	2160 …90000	60	this work	1.42e-7	0.9999837

Table 4: Omission error from topographic potential degree variances (based on spherical approximation) computed in this study from GGMplus tiles and from popular degree variance models for various degree ranges in terms of geoid heights [m] and gravity disturbances [mGal]

Degree variance model Truncation at	***Underlying data***	***2161 – 90,000 2160***		***10,801 – 90,000 10,800***		***21,601 – 90,000 21,600***	
		[mGal]	**[cm]**	**[mGal]**	**[cm]**	**[mGal]**	**[cm]**
Kaula : c_K^2	Space gravity	23.93	2.64	18.05	0.52	14.81	0.26
Tscherning/Rapp : c_{TRorig}^2	1° free-air gravity	11.18	2.31	1.17	0.06	0.11	~3e-3
Sanso/Sideris : c_{SS}^2	EGM2008	1.38	0.32	0.03	~2e-3	~9e-4	~2e-5
corrected Sanso/Sideris : c_{SS}^2	EGM2008	3.12	0.64	0.56	0.02	0.12	~3e-3
This work (average of all 2.5° tiles, all types of terrain)	GGMplus	8.62	1.53	3.51	0.13	2.23	0.02
Terrain RMS = 0 – 250m	GGMplus	2.77	0.48	1.23	0.04	0.84	0.01
Terrain RMS = 250 – 500 m	GGMplus	3.95	0.70	1.68	0.06	1.10	0.02
Terrain RMS = 500 – 750 m	GGMplus	6.33	1.13	2.59	0.10	1.64	0.03
Terrain RMS = 750 – 1000 m	GGMplus	8.83	1.58	3.54	0.14	2.21	0.04
Terrain RMS = 1000 – 2000 m	GGMplus	10.93	1.96	4.29	0.17	2.63	0.05
Terrain RMS = 2000 – 3000 m	GGMplus	16.31	2.94	6.35	0.25	3.87	0.08
Terrain RMS > 3000 m	GGMplus	23.31	4.24	8.66	0.34	5.06	0.11
Maximum values of all 2.5° tiles (located in the Himalayas)	GGMplus	38.13	7.51	14.9	0.62	9.11	0.2

GGMplus-based omission errors

Looking at the GGMplus-based omission errors (computed as averages over all 2.5° tiles) we find the signal strengths of omitted signals on the order of ~ 9 mGal for gravity (~1.5 cm for geoid effects) at scales of ~10 km, ~ 4 mGal (~ 1 mm) at scales of ~ 2km and ~ 2 mGal (~ 0.2mm) at scales of ~ 1km. Our omission errors are lower than those of Kaula's rule and somewhat

higher than those based on the Tscherning/Rapp (1974) degree variance model beyond degree 10800 (Table 4).

Correction to Sanso and Sideris (2013)

The Sanso and Sideris (2013) degree variance model based on their numerical values $A = 3.9 \cdot 10^{-8}$ and $B = 0.999443$ (solid grey line) is shown in Fig. 12. This model is in clear disagreement with the EGM2008 spectrum. Instead, a least-squares fit of the EGM2008 degree variances is obtained with Sanso and Sideris' model along with coefficients $A = 5.0 \cdot 10^{-8}$ and $B = 0.999845$ (dashed grey line). We denote this as "corrected Sanso and Sideris model". Note that while the numerical coefficients listed in Sanso and Sideris (2013) are not correct, their figures and omission error estimates seem to be based on coefficients similar to our corrected model.

Ellipsoidal approximation underestimates omission errors

Importantly, the GGMplus omission error estimates are considerably larger than those based on EGM2008 spherical harmonic potential coefficients. Omission errors thus appear to be much underestimated in ellipsoidal approximation. For instance, the omission error beyond degree 2160 seemingly reduces from ~1.5 cm for GGMplus to ~0.6 cm (~0.3 cm) for the corrected (original) Sanso and Sideris model by virtue of the approximation level. This effect is much more pronounced for ultra-short scales, e.g., ~2.2 mGal (from GGMplus) versus ~0.12 mGal signal strength (corrected Sanso and Sideris model) beyond degree 21,600.

These results – to our understanding – show that the ellipsoidal approximation level of the spherical harmonic spectra is not compatible with the spherical computation of omission errors. This is corroborated by the observation that a ~0.6 cm geoid omission error for degree 2160 expansions is in contrast to practical results from omission error modelling (e.g., Jekeli et al. 2009; Hirt et al. 2010) showing this effect to be on the lower cm-level. Using models of spherical approximation type yields more realistic estimates of the short-scale spectral energy (e.g., Tscherning/Rapp: 2.3 cm, this work: 1.5 cm geoid signals) omitted by degree-2160 expansions. Another way to obtain realistic estimates of short-scale spectral energy would be to work entirely with ellipsoidal harmonics. The spectral energy of spherical harmonic models in spherical approximation is very close to the energy of the truly ellipsoidal harmonic spectrum (compare e.g. to Fig. 7, p. 24 in Pavlis et al. 2012).

On the other hand, EGM2008 represents truly global degree variances, while the GGMplus variances are only valid over land, where the gravity field power was shown to be larger than globally. As such, one would expect the true (albeit unknown) omission error to be somewhat lower than that derived from the GGMplus land data.

GGMplus-based omission errors for different types of terrain

Investigation of the omission error dependence on the Terrain RMS present in the tiles exhibits an increase in omission error with rising terrain elevation (Table 4). As expected the error produced by the truncation of the spherical harmonic series at some degree > 2160 in average is larger in regions of large topographic masses (Terrain RMS = 7) than in low elevated regions (Terrain RMS = 1). Although the gravity signal beyond degree ~21600 becomes small

(~2mGal and <1 mm) on average, there are regions on Earth where there is still significant contribution of topographic masses to the gravity signal. This can be concluded from the maximum omission error of all 1502 2.5° tiles per degree (bottom row in Table 4), which is found in the Himalayas (75°E to 77.5°E and 32.5°N to 35°N). The investigation of the maxima indicates that at scales less than ~1 km (degree 21600) the omission error can still be on the order of 9 - 10 mGal (~ 2 mm) over high elevated areas (bottom rows in Table 4).

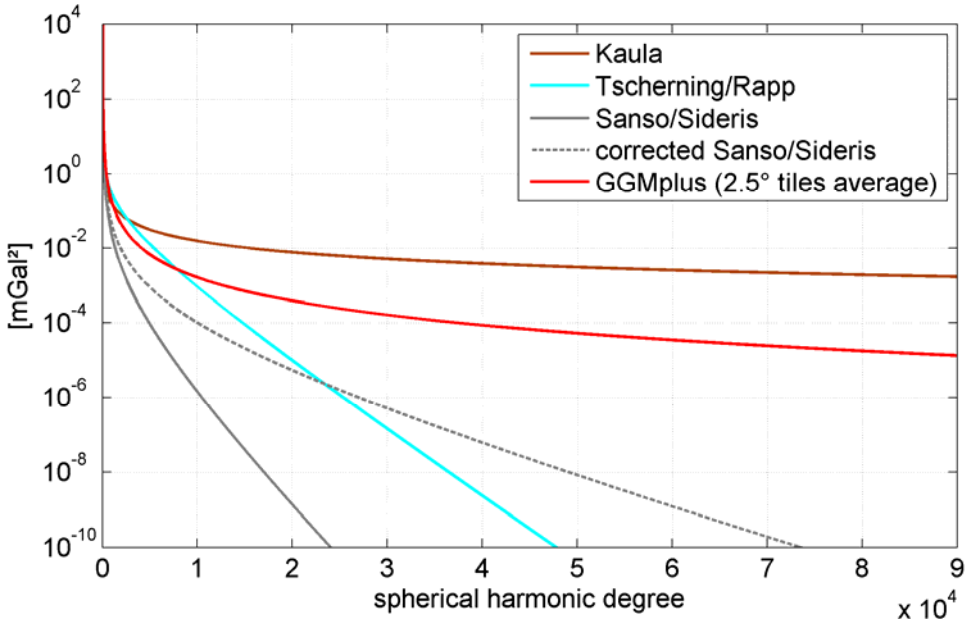

Figure 13: Overview on computed GGMPlus degree variances and selected well-known degree variances (from models) in terms of gravity disturbances [mGal²]

Corroboration from dV-SPH-RET2012

The GGMplus degree variances are in close agreement with those from the topographic potential dV-SPH-RET2012 (2D-DFT recovered using a similar area as GGMplus) at short spatial scales, and nearly coincide at degree 2160 (compare solid red and dashed blue lines in Fig. 13). The dashed blue line and the red line express signal strengths of the same gravity functional (gravity disturbances from topographic potential model evaluated at the top of the topography) and over the same region of Earth. Given that a large part of Earth's observed gravity field (i.e., GGMplus to degree 2160) is generated by the topographic masses at short scales, this good agreement between the 2D-DFT-recovered dV-SPH-RET2012 and GGMplus is within the expectations, and indicates the consistency of our processing procedure.

Validation with Parseval's Theorem

The validity of our processing is assessed by evaluating Parseval's theorem that states identical signal power in space and frequency domain and, hence, a lossless transformation between the domains (see e.g. Papoulis 1984). Parseval's Theorem in our case can be written as

$$\sqrt{\int_{0}^{360}\int_{-90}^{90} |f(\varphi,\lambda)|^2 \cos\phi \;\mathrm{d}\phi \;\mathrm{d}\lambda} = \sqrt{\int_{n_{min}}^{n_{max}} c_n(l)^2 \,\mathrm{dl}} \qquad (28)$$

where in our discrete case the left hand side is equivalent to the root-mean-square of the function $f(\varphi, \lambda)$ (in space domain), here given on a grid, and the right hand side corresponds to the omission error (in frequency domain). From Hirt et al. (2014), Table 3 ibid, the total RMS of GGMplus gravity and geoid effects at spatial scales of ~10 km to 220 m (where the model relies on topography-implied gravity only) is 1.6 cm in geoid height (10.59 mGal) in the space domain (left side of Eq. 28). This is in good agreement to the omission error from the 2D-DFT recovered GGMplus spectrum of 1.51 cm (8.62 mGal) from our computed degree variances for the degree range 2161…90,000 (right side of Eq. 28). The differences are less than 20% (gravity) and below 10% (geoid), which is commensurate to the approximation errors of the 2D-DFT method quantified in Sect. 3.

Comparison with classical degree variance models at ultra-short scales

Comparing all degree variance models in the short and the ultra-short wavelengths (Fig. 13) reveals strong divergence. This is not surprising as the classical degree variance models were developed based on long/medium-wavelength gravity data, so are extreme extrapolations in the ultra-high degrees. Beyond degree 8000 Kaula's rule shows the least decay, while the Tscherning/Rapp model indicate much faster decay of the gravity signal. The GGMplus derived signal (representing continental, forward modelled gravity as synthesised on top of the topography) resides in between those of the classical models. Of all degree variance models in Fig. 13, it is only the GGMplus based spectrum that is supported by gravity data (topography-implied) to ultra-fine scales of degree 90,000.

The extrapolation effect of the classical models at ultra-short scales is evident e.g., from estimated omission errors beyond degree 21600, where the Tscherning-Rapp model suggest 0.11 mGal gravity signal strengths which is a factor as large as 20 below those indicated by the GGMplus-based spectrum (2.2 mGal, cf. Table 4). Conversely, Kaula's rule significantly overestimates the gravity signal omission at these scales by a factor of 7 compared to GGMplus (cf. Table 4).

Comparison with literature results

Finally, comparing the estimated (spherical) omission errors from our new degree variance model (Table 4) with previous regional work we find our values in the same magnitude range. Voigt and Denker (2007) have estimated the omission error from RTM gravity effects in three 1° x 1° bins in Germany (German Alps, Harz and Franconia), representing rough and rather smooth topographic areas. In those areas the omission error at degree 10800 in terms of geoid heights ranges from 0.1 cm to 0.5 cm (this work: ~ 0.13 cm in average, ranging from 0.04 cm to 0.34 cm). For degree 21600 their analyses yield a geoid RMS power of 0.0 cm to 0.1 cm (this work: ~0.045 cm in average, ranging from 0.01 cm to 0.1 cm).

5. Summary and outlook

This study started with some remarks on topographic gravity modelling and recapitulating the definition and meaning of degree variances and current degree variance models. For the approximation of signal powers of Earth's topographic potential from gridded gravitational field quantities in terms of degree variances we describe and investigate the 2D-DFT approach

dating back to Forsberg (1984a) and Flury (2006) and discussed curve fitting based on the analytical functions of common degree variance models. Closed-loop experiments with the 2D-DFT approach on global scale revealed that:

(i) the approach can be used for recovery of degree variances with 10 – 20 % accuracy;
(ii) this holds true also for tiling of the global grid and consecutive averaging (and fitting) of the degree variances obtained in each tile;
(iii) the tiling and averaging leads to an oscillation of the signal around the original degree variance; the oscillation's frequency and magnitude is linked to the tile size;
(iv) the azimuth averaging procedure determines the smoothness and the spectral resolution of the computed degree variances.

As key result of this work, we applied the 2D-DFT procedure to GGMplus gravity maps, yielding a new degree variance model for gravity signal strengths at the surface of the topography:

$$c^2_{GGMplus}(l) = \frac{1.79 \cdot 10^{-7} \cdot (0.999995)^l}{(l-1)(l-2)(l+4)(l+17)} \quad (29)$$

This model is supported by about 3 billion points of GGMplus topography-implied gravity effects at spatial scales of 10 km to 220 m over all land areas where SRTM data is available. The model is thus defined for harmonic degrees up to 90,000 and allows for estimates of omission errors that are in the order of ~ 9 mGal (~1.5 cm) at scales of ~10 km (degree 2160 truncations), and ~ 3.5 mGal (~ 1 mm) at scales of ~ 2km (degree 10,800 truncations). The approximation errors caused by the 2D-DFT procedure (instead of rigorous spherical harmonic modelling) was found to be 20% or less.

In comparison to degree variance models fitted to spectra of spherical harmonic coefficients/ geopotential models, the model in Eq. (29) has two major differences that make it incompatible to those (apart from the fact that the input GGMplus gravity data is not truly global).

First, it does not describe signal strengths of gravity downward-continued (amplified) to some reference surface (which is the case in spherical harmonic models of the topographic and gravitational potential). Instead, our new degree variance model describes gravity signal strengths as found at the surface of the topography. This is compatible with signal strengths of (unreduced in the sense of not continued) terrestrial gravity field observations and represents a more natural way for describing short-scale signal characteristics.

Second, the new degree variance model reflects a spherical approximation of the field-generating masses. It is thus not compatible with spherical harmonic degree variance models from geopotential models that reflect the field generating masses to be – in good approximation - ellipsoidal. Importantly, degree variance models relying on ellipsoidal approximation were shown to underestimate the spectral energy of gravity at short spatial scales. They therefore lead to unrealistically small omission errors. In this context an empirical rule has been developed to transform spherical harmonic spectra between spherical and

ellipsoidal approximation. The spherical harmonic spectrum in spherical mass approximation is found to be very close to a truly ellipsoidal harmonic spectrum.

While building upon approximations and assumptions, it is hoped that the new GGMplus-based degree variance model provides an improved description of the Earth's gravity spectrum to ultra-fine spatial scales. Refining the chosen 2D-DFT approach through a more sophisticated estimation of the localized power spectrum, e.g. by multitaper spectral methods / Slepian tapers (e.g. Dahlen and Simons 2008, Szücs 2014) and a more rigorous analysis of approximation errors warrant future research. It is also likely that in the next years spherical harmonic analysis procedures will be used up to ultra-short scales, yielding further improved estimates of the signal power at those scales in a truly global manner.

Acknowledgments

With the support of the Technische Universität München – Institute for Advanced Study, funded by the German Excellence Initiative. We thank the Australian Research Council for funding via grant DP120102441. We thank Roland Pail for sharing his knowledge on Fourier transforms, Reiner Rummel for directing us to Parseval's theorem, and Sten Claessens for the discussions related to degree variances. We are grateful for very constructive and thorough reviews received from four anonymous reviewers, improving the clarity of presentation and stimulating future research.

References

Abrykosov O, Förste C, Gruber C, Shako R, Barthelmes F (2012) Harmonic analysis of the DTU10 global gravity anomalies. In: Abbasi A, Giesen N (eds) EGU General Assembly Conference Abstracts, EGU General Assembly Conference Abstracts, vol 14, p 4945

Balmino G, Vales N, Bonvalot S, Briais A (2012) Spherical harmonic modelling to ultra-high degree of Bouguer and Isostatic anomalies. Journal of Geodesy 86(7):499–520, DOI10.1007/s00190-011-0533-4

Claessens S, Hirt C (2013) Ellipsoidal topographic potential - new solutions for spectral forward gravity modelling of topography with respect to a reference ellipsoid. Journal of Geophysical Research 118 (11): 5991–6002, DOI 10.1002/2013JB010457

Dahlen FA, Simons FJ (2008) Spectral estimation on a sphere in geophysics and cosmology. Geophysical Journal International 147:774-807, DOI 10.1111/j.1365-246X.2008.03854.x

Farr T, Rosen P, Caro E, Crippen R, Duren R, Hensley S, Kobrick M, Paller M, Rodriguez E, Roth L, Seal D, Shaffer S, Shimada K, Umland J, Werner M, Oskin M, Burbank D, Alsdorf D (2007) The Shuttle Radar Topography Mission. Reviews of Geophysics 45 (RG2004), DOI 10.1029/2005RG000183

Flury J (2006) Short-wavelength spectral properties of the gravity field from a range of regional data sets. Journal of Geodesy 79:624–640, DOI 10.1007/s00190-005-0011-y

Forsberg R (1984a) Local Covariance Functions and Density Distribution. OSU Report 356, Ohio State University

Forsberg R (1984b) A study of terrain reductions, density anomalies and geophysical inversion methods in gravity field modelling. OSU Report 355, Ohio State University

Grombein T, Luo X, Seitz K, Heck B (2014) A wavelet-based assessment of topographic-isostatic reductions for goce gravity gradients. Surveys in Geophysics pp 1–24, DOI 10.1007/s10712-014-9283-1

Gruber C, Abrikosov O (2014) High resolution spherical and ellipsoidal harmonic expansions by Fast Fourier Transform. Studia Geophysica et Geodaetica 58, online first, DOI: 10.1007/s11200-013-0578-3

Heller W, Jordan S (1976) A new self-consistent statistical gravity field model. In: Eos Trans. AGU Fall Meeting, San Francisco, vol 75, p. 895

Hirt C (2012) Efficient and accurate high-degree spherical harmonic synthesis of gravity field functionals at the Earth's surface using the gradient approach. Journal of Geodesy 86(9):729–744, DOI: 10.1007/s00190-012-0050-y

Hirt C, Kuhn M (2012) Evaluation of high-degree series expansions of the topographic potential to higher-order powers. Journal of Geophysical Research Solid Earth 117, DOI 10.1029/22012JB009492

Hirt C, Kuhn M (2014) A band-limited topographic mass distribution generates a full-spectrum gravity field - gravity forward modelling in the spectral and spatial domain revisited. Journal of Geophysical Research - Solid Earth 119, DOI:10.1002/2013JB010900

Hirt C., M. Kuhn, S.J. Claessens, R. Pail, K. Seitz, T. Gruber (2014), Study of the Earth's short-scale gravity field using the ERTM2160 gravity model, Computers & Geosciences, 73, 71-80, DOI: 10.1016/j.cageo.2014.09.00

Hirt C, Featherstone W, Marti U (2010) Combining EGM2008 and SRTM/DTM2006.0 residual terrain model data to improve quasigeoid computations in mountainous areas devoid of gravity data. Journal of Geodesy 84(9):557–567, DOI: 10.1007/s00190-010-0395-1

Hirt C, Claessens S, Fecher T, Kuhn M, Pail R, Rexer M (2013) New ultra-high resolution picture of Earth's gravity field. Geophysical Research Letters 40(16), 4279-4283, DOI: 10.1002/grl.50838

Holmes S, Pavlis N (2008) EGM Harmonic Synthesis Software. , National Geospatial-Intelligence Agency, http://earth-info.nga.mil/GandG/wgs84/gravitymod/ new egm/new egm.html

Jekeli C (1978) An investigation of two models for the degree variances of global covariance functions. OSU 275, Department of Geodetic Science, Ohio State University

Jekeli C, Yanh HJ, Kwon JH (2009) Evaluation of EGM08 - globally and locally in South Korea. Newton's Bulletin pp 38–49

Jekeli C (2010) Correlation Modeling of the Gravity Field in Classical Geodesy. In: Freeden W, Nashed M, Sonar T (eds) Handbook of the Geomathematics, Springer-Verlag Berlin Heidelberg, DOI 10.1007/978-3-642-01546-5 28

Kaula W (1966) Theory of Satellite Geodesy. Blaisdel, Waltham

Kuhn M, Seitz K (2005) Comparison of Newton's integral in the space and frequency domains. In: Sanso F (ed) A window on the Future of Geodesy - IAG Symposia, vol 128, pp 386–391

Mayer-Gürr T, Kurtenbach E, Eicker A (2010) ITG-Grace2010 Gravity Field Model. , www.igg.unibonn.de/apmg/index.php?id=itg-grace2010

Moritz H (1977) On the computation of a global covariance model. OSU 255, Department of Geodetic Science, Ohio State University

Moritz H (2000) Geodetic Reference System 1980. Journal of Geodesy 74(1):128–162, DOI : 10.1007/s001900050278

Novak P (2010) Direct modelling of the gravitational field using harmonic series. Acta Geodyn Geomater 7(1 (157)):35–47

Pail R, Goiginger H, Mayrhofer R, Schuh WD, Brockmann JM, et al (2010) GOCE gravity field model derived from orbit and gradiometry data applying the Time-Wise Method. Proc ESA Living Planet Symp 28.June-2.July (ESA SP-686)

Pail R, Bruinsma S, Migliaccio F, Förste C, Goiginger H, Schuh WD, Höck E, Reguzzoni M, Brockmann JM, Abrikosov O, Veicherts M, Fecher T, Mayrhofer R, Krasbutter I, Sanso F, Tscherning CC (2011) First GOCE gravity field models

derived by three different approaches. Journal of Geodesy 85(11):819–843, DOI 10.1007/s00190-011-0467-x, special issue: ”GOCE - The Gravity and Steady-state Ocean Circulation Explorer”

Papoulis A (1984) Signal Analysis. McGraw-Hil Book Company

Pavlis, N. K. and Rapp, R. H. (1990), The development of an isostatic gravitational model to degree 360 and its use in global gravity modelling. Geophysical Journal International, 100: 369–378. doi: 10.1111/j.1365-246X.1990.tb00691.x

Pavlis N, Factor J, Holmes S (2007) Terrain-related gravimetric quantities computed for the next EGM. In: Dergisi H (ed) Proceedings of the 1st International Symposium of the International Gravity Field Service, vol 18, pp 318–323

Pavlis N, Holmes S, Kenyon S, Factor J (2012) The development and evaluation of the Earth Gravitational Model 2008 (EGM2008). Journal of Geophysical Research 117, DOI 10.1029/2011JB008916

Rexer M, Hirt C (2014) Comparison of free high resolution digital elevation data sets (ASTER GDEM2, SRTM v2.1/v4.1) and validation against accurate heights from the Australian National Gravity Database. Australian Journal of Earth Sciences 0(0):1–15, DOI 10.1080/08120099.2014. 884983, URL http://www.tandfonline.com/doi/abs/10.1080/08120099.2014.884983

Rummel R, Rapp R, Sünkel H, Tscherning C (1988) Comparisons of Global Topographic/ Isostatic Models To the Earth’s Observed Gravity Field. OSU report 388, Ohio State University

Sanso F, Sideris M (2013) Geoid Determination - Lecture Notes in Earth Sciences, vol 110, Springer-Verlag Berlin Heidelberg, chap Harmonic Calculus and Global Gravity Models

Szücs E, Papp G, Benedek J (2014) A study of different wavelength spectral components of the gravity field derived from various terrestrial data sets, Acta Geodaetica et Geophysica, online first, DOI 10.1007/s40328-014-0061-9

Tapley BD, Bettadpur S, Watkins M, Reigber C (2004) The gravity recovery and climate experiment: Mission overview and early results. Geophys. Res. Lett., 31, L09607, *DOI* 10.1029/2004GL019920.

Torge W (2001) Geodesy, 3rd edn. Walter de Gruyter

Tscherning C, Rapp R (1974) Closed covariance expressions for gravity anomalies, geoid undulations, and deflections from the vertical implied by anomaly degree variance models. 208, Ohio State University

Vassiliou A, Schwarz K (1987) Study of the high-frequency spectrum of the anomalous potential, Journal of Geophysical Research 92(B1), 609-617

Voigt C, Denker H (2007) A study of high frequency terrain effects in gravity field modelling. In: Dergisi H (ed) 1st International Symposium of the INternational Gravity Field Service, ”Gravity Field of the Earth”, Ankara, Turkey, vol 18, pp 342–347

Wenzel H, Arabelos D (1981) Zur Schätzung von Anomalie-Gradvarianzen aus lokalen empirischen Kovarianzfunktionen. Zeitschrift für Vermessungswesen 106:234–243